

VILNIUS UNIVERSITY
CENTER FOR PHYSICAL SCIENCES AND TECHNOLOGIES

EDITA PALAIMIENE

BROADBAND DIELECTRIC SPECTROSCOPY OF RELAXOR AND
RELATED CERAMICS

Doctoral dissertation
Physical sciences, Physics (02P)

Vilnius 2017

The dissertation was prepared at Vilnius University in 2011 – 2016.

Academic supervisor - prof. habil. dr. Juras Banys (Vilnius University, physical sciences, physics – 02P).

The dissertation will be defended at joint scientific council of Vilnius University and Center for Physical Sciences and Technology:

Chairman - prof. habil. dr. Vytautas Balevicius (Vilnius University, physical sciences, physics – 02P);

Members:

prof. habil. dr. Antanas Feliksas Orliukas (Vilnius University, physical sciences, physics – 02P);

prof. dr. Valdas Sablinskas (Vilnius University, physical sciences, physics – 02P);

prof. habil. dr. Donatas Rimantas Vaisnoras (Lithuanian University of Educational Sciences, physical sciences, physics – 02 P);

dr. Janis Kleperis (University of Latvia, Latvia, physical sciences, physics – 02P).

The dissertation will be defended at public meeting of joint scientific council of Vilnius University and Center for Physical Sciences and Technologies on 17nd February 2017 at 15.00 in auditorium 815, Faculty of Physics, Vilnius University.

Address: Sauletekio av. 9, III bld., LT-10222, Vilnius, Lithuania.

The summary of doctoral dissertation was distributed on 17nd January 2017.

The dissertation is available at the libraries of VU, CPST and at website: www.vu.lt/lt/naujienos/ivykiu-kalendorius.

VILNIAUS UNIVERSITETAS
FIZINIŲ IR TECHNOLOGIJOS MOKSLŲ CENTRAS

EDITA PALAIMIENĖ

PLAČIADAŽNĖ RELAKSORIŲ IR GIMINIGŲ KERAMIKŲ DIELEKTRINĖ
SPEKTROSKOPIJA

Daktaro disertacija
Fiziniai mokslai, fizika (02 P)

Vilnius 2017

Disertacija rengta 2011 – 2016 metais Vilniaus universitete.

Mokslinis vadovas - prof. habil. dr. Jūras Banys (Vilniaus universitetas, fiziniai mokslai, fizika – 02 P).

Disertacija ginama jungtinėje VU ir FTMC Fizikos mokslo krypties taryboje:

Pirmininkas – prof. habil. dr. Vytautas Balevičius (Vilniaus universitetas, fiziniai mokslai, fizika – 02 P).

Nariai:

prof. habil. dr. Antanas Feliksas Orliukas (Vilniaus universitetas, fiziniai mokslai, fizika – 02 P);

prof. dr. Valdas Šablinskas (Vilniaus universitetas, fiziniai mokslai, fizika – 02 P);

prof. habil. dr. Donatas Rimantas Vaišnoras (Lietuvos edukologijos universitetas, fiziniai mokslai, fizika – 02 P);

dr. Janis Kleperis (Latvijos universiteto Kietojo kūno fizikos institutas, Latvija, fiziniai mokslai, fizika – 02P).

Disertacija bus ginama viešame Fizikos mokslo krypties tarybos posėdyje 2017 m. vasario mėn. 17 d. 15:00 val. Fizikos fakulteto 815 auditorijoje. Adresas: Saulėtekio al. 9-III, LT-10222 Vilnius, Lietuva.

Disertacijos santrauka išsiuntinėta 2017 m. sausio mėn. 17 d.

Disertaciją galima peržiūrėti Vilniaus universiteto, Fizinių ir technologijos mokslų centro bibliotekose ir Vilniaus universiteto interneto svetainėje adresu: www.vu.lt/lt/naujienos/ivykiu-kalendorius.

CONTENTS

1. INTRODUCTION	6
SCIENTIFIC NOVELTY	6
THE MAIN AIM AND TASKS OF THIS THESIS	7
STATEMENTS PRESENTED FOR DEFENSE	8
STRUCTURE OF THE THESIS	9
2. LITERATURE REVIEW	9
3. EXPERIMENTAL METHOD	12
4. RESULTS AND DISCUSSIONS	12
4.1. PMT-PT crystals	12
4.2. $\text{Bi}_{1-x}\text{Sm}_x\text{FeO}_3$ ceramics.....	16
4.3. $\text{Bi}_{1-x}\text{Dy}_x\text{FeO}_3$ ceramics	18
4.4. $\text{Bi}_{4-x}\text{Gd}_x\text{Ti}_3\text{O}_{12}$ ceramics.....	20
4.5. $\text{Ba}_{6-2x}\text{Nd}_{2x}\text{Fe}_{1+x}\text{Nb}_{9-x}\text{O}_{30}$ ceramics	23
4.6. $\text{Ba}_2\text{NdFeNb}_{4-x}\text{Ta}_x\text{O}_{15}$ ceramics	27
5. CONCLUCIONS	30
REFERENCES	32
AUTHOR’S PUBLICATION LIST	34
PARTICIPATION IN CONFERENCES.....	34

1. INTRODUCTION

Advanced materials are necessary for development of telecommunications, information technology and electronics. High requirements apply for new materials, for example, dielectric permittivity value, low losses, easy production and the best price-performance ratio. Ferroelectrics and related materials, such as ferroelectric relaxors and thin layers thereof, are materials which have unique dielectric and piezo properties. Although a number of ferroelectrics compounds have already been discovered, microscopic mechanisms of ferroelectricity have not yet been worked out in detail. Furthermore, modifications are often necessary for the practical use of ferroelectrics with adding impurities or changing the dimensions of the structures (for example, the thickness of the layer). Such modification is hardly predictable, therefore, ferroelectrics, relaxors and related materials are subjects of intense research. Every material has different features, which have to be investigated with different techniques. The broadband dielectric spectroscopy is a powerful tool for investigating various materials. It enables not only to detect the dielectric strength and the amount of losses at various frequencies but also to determine the characteristic relaxation time, their distribution and the phase diagram of a material.

Unique feature combinations occur in multiferroic compounds or simply multiferroics. Recently, tetragonal tungsten bronze (TTB) family materials have received a lot of attention. Three types of sites existing between oxygen octahedron allows for the insertion of different ions not only to these sites but also to same octahedrons and to get materials with various phase diagrams.

SCIENTIFIC NOVELTY

Ferroelectric relaxor $0.94\text{PbMg}_{1/3}\text{Ta}_{2/3}\text{O}_3 - 0.06\text{PbTiO}_3$ (PMT-PT) possess interesting features. The aim of the investigation of this crystal is to find out more about ferroelectric relaxor features, particularly about the static permittivity behaviour at higher temperatures.

Recently a lot of attention has been paid to bismuth ferrite because of its ferroelectric and magnetic characteristics' coexistence. However, the properties of pure

bismuth ferrite are not good for application, because this material has a strong leakage current. In order to improve the properties of this material the part of bismuth is replaced with other rare earth elements (e.g. Nd, La, Sm, Dy). Samarium and dysprosium are one of options for such replacement; by changing the concentration of these elements it might be possible to improve the properties. However, the addition of impurities to ferroelectrics can cause some unwanted scenarios, for example, the loss of the ferroelectric properties or an undesirable dipolar glass phase or relaxor phase. The broadband dielectric spectroscopy is an excellent tool for the research of dielectric properties in a broad frequency range. In this thesis it is shown for the first time that in $\text{Bi}_{1-x}\text{Sm}_x\text{FeO}_3$ ceramics when $x = 0.2$ ferroelectric properties disappear and relaxor phase occurs, while ferroelectric properties in $\text{Bi}_{1-x}\text{Dy}_x\text{FeO}_3$ ceramics remain even when $x = 0.2$ and the dielectric losses decrease with dysprosium concentration.

Multiferroic materials with Aurivillius structure are also interesting, particularly materials based on $\text{Bi}_4\text{Ti}_3\text{O}_{12}$ (BIT). BIT has a high Curie temperature (943 K) that makes BIT widely used in electrical elements such as energy converters or piezo-electric memory devices. To obtain multiferroic material the attempts to dope BIT with rare earth metals with magnetic properties (for example gadolinium) were made. In this work dielectric investigations of $\text{Bi}_4\text{Ti}_3\text{O}_{12}$ and $\text{Bi}_{4-x}\text{Gd}_x\text{Ti}_3\text{O}_{12}$ (BGT) ($x = 1$ and $x = 1.5$) are presented. It is shown that the ferroelectric order does not disappear in BGT with $x = 1.5$ and the dielectric dispersion is determined by ferroelectric domain dynamics.

Recently TTB materials family has been receiving increasingly more attention. $\text{Ba}_2\text{REFeNb}_4\text{O}_{15}$ (RE = La, Pr, Nd, Sm, Eu, Gd) is a great example of diverse TTB properties. Although compounds with neodymium, samarium and europium are ferroelectrics, ceramics with praseodymium and gadolinium exhibit ferroelectric relaxor properties, there has been a lack of broadband dielectric investigations of these materials. This work investigated dielectric properties and phase diagrams of $\text{Ba}_2\text{NdFeNb}_4\text{O}_{15}$, $\text{Ba}_{6-2x}\text{Nd}_{2x}\text{Fe}_{1+x}\text{Nb}_{9-x}\text{O}_{30}$ ($x = 0.6, 0.8$), $\text{Ba}_2\text{NdFeNb}_{4-x}\text{Ta}_x\text{O}_{15}$ ($x = 0.3, 0.6, 2$).

THE MAIN AIM AND TASKS OF THE THESIS

Main purpose of the work was to investigate the influence of impurities on dielectric and electric properties of various ferroelectrics and relaxors.

The main tasks were the following:

- To investigate dielectric and electric properties of $0.94\text{PbMg}_{1/3}\text{Ta}_{2/3}\text{O}_3 - 0.06\text{PbTiO}_3$, $\text{Bi}_{1-x}\text{RE}_x\text{FeO}_3$ (RE = Sm, Dy), $\text{Bi}_{4-x}\text{Gd}_x\text{Ti}_3\text{O}_{12}$, $\text{Ba}_{6-2x}\text{Nd}_{2x}\text{Fe}_{1+x}\text{Nb}_{9-x}\text{O}_{30}$, $\text{Ba}_2\text{NdFeNb}_{4-x}\text{Ta}_x\text{O}_{15}$ materials in wide temperature and frequency ranges.
- To explain the temperature dependence of the static dielectric permittivity of $0.94\text{PbMg}_{1/3}\text{Ta}_{2/3}\text{O}_3 - 0.06\text{PbTiO}_3$ crystals.
- To investigate the phase diagram of BiFeO_3 with of samarium ($0.1 \leq x \leq 0.2$).
- To investigate the influence of samarium ($0.1 \leq x \leq 0.2$) and dysprosium ($0.1 \leq x \leq 0.2$) on electrical conductivity of BiFeO_3 .
- To investigate the influence of gadolinium ($0 \leq x \leq 1.5$) on electrical conductivity of $\text{Bi}_4\text{Ti}_3\text{O}_{12}$.
- To determine the phase diagram of $\text{Ba}_{6-2x}\text{Nd}_{2x}\text{Fe}_{1+x}\text{Nb}_{9-x}\text{O}_{30}$ and $\text{Ba}_2\text{NdFeNb}_{4-x}\text{Ta}_x\text{O}_{15}$ ceramics.

STATEMENTS PRESENTED FOR DEFENSE

- 1) The static dielectric permittivity temperature dependence of PMT-PT crystal can be described by Spherical Random-Bond–Random-Field model.
- 2) The ferroelectric phase transition temperature increases with bismuth concentration in $\text{Bi}_{1-x}\text{Sm}_x\text{FeO}_3$ ceramics, a typical ferroelectric relaxor behaviour is observed for $x = 0.2$. $\text{Bi}_{0.85}\text{Sm}_{0.15}\text{FeO}_3$ ceramics exhibit antiferroelectric phase transition.
- 3) In $\text{Ba}_2\text{NdFeNb}_{4-x}\text{Ta}_x\text{O}_{15}$ ceramics for $x \leq 0.30$, the coexistence of the ferroelectric and relaxor states is observed at low temperatures. Only a typical relaxor behaviour is observed for $x \geq 0.30$.

AUTHOR'S CONTRIBUTION

The author of the dissertation performed all dielectric tests, carried out an analysis of the data and summarized the results. The author published research articles, also

prepared verbal reports and poster presentations for conferences. Most of them were presented by herself.

STRUCTURE OF THE THESIS

The dissertation contains five chapters. It consists of 115 pages, 3 tables, 84 images and 97 literature references.

The first chapter is an introduction where the importance of dissertation, the aim and the tasks, the obtained scientific novelty of the results and the statements for defence are presented. Also the list of articles and theses on the topic of the dissertation which were published in various national and international conferences and seminars are presented. The second chapter reviews the literature on ferroelectrics and ferroelectric relaxors, tested materials properties published in other author's works. The third chapter describes experimental methods applied while preparing the dissertation. The fourth chapter provides and discusses the results of the doctoral studies. The fifth chapter provides the conclusions of the thesis. The list of references is provided at the end of the dissertation work.

2. LITERATURE REVIEW

Relaxor ferroelectrics were discovered almost 50 years ago among the complex oxides with perovskite structure [1]. PMT ceramic dielectric spectra were explored in these different references [2, 3, 4]. One of the earliest investigations of PMT properties is presented in [3]. The PMT ceramics exhibit relaxor ferroelectric behaviour with a relative permittivity maximum of 5100 at 188 K at 1 kHz [2, 3, 4]. X-ray diffraction tests showed that at room temperature $\text{PbMg}_{1/3}\text{Ta}_{2/3}\text{O}_3$ (PMT) exhibits the cubic symmetry [5]. Single crystals of PMT–PT of concentration $0 \leq x \leq 0.6$ dielectric studies showed that with Ti concentration increase the observed phase transition transforms gradually from the relaxor type to normal ferroelectric one and shifts towards higher temperatures, and this is of phase transition nature from the relaxor behaviour for PMT to the normal ferroelectric one for 0.4PMT–0.6PT [6, 7]. X-ray tests showed that PMT-PT crystals are of the perovskite

structure and the room temperature symmetry in the series $(1-x)\text{PbMg}_{1/3}\text{Ta}_{2/3}\text{O}_3-x\text{PbTiO}_3$ or $(1-x)\text{PMT}-x\text{PT}$ or PMT-PT changes from the cubic to the tetragonal [6, 7, 8].

Among the multiferroic materials, BiFeO_3 (BFO) is a unique material exhibiting ferroelectric and antiferromagnetic orders at room temperature (the Neel temperature is about 643 K, the ferroelectric Curie temperature is about 1103 K) [9]. Although this material has a great potential, it encountered problems in combination of magnetic and ferroelectric properties, because they need the symmetry which is hardly compatible in terms of both properties; therefore a certain compromise should be reached. This compromise can be arrived at by adding rare earth elements (for example, Nd, La, Sm, Dy), which accentuate multiferroic properties. The properties of BFO based materials is the object of many investigations due to an attractive coexistence of ferroelectric and magnetic properties. However, dielectric investigations of these materials are rare enough, particularly in wide frequency range. The work [10] can be distinguished which established that in BFO ceramics, below 175 K, the sum of polar phonon contributions to the permittivity corresponds to the value of the permittivity at 1 MHz while at higher temperatures, a giant low-frequency permittivity was observed, obviously due to the enhanced conductivity and possible Maxwell-Wagner contribution. In BFO ceramic the dielectric dispersion is highly dependent on the conditions of production, which have the impact on the conduction phenomena and dielectric permittivity value [9, 11, 12, 13]. $\text{Bi}_{1-x}\text{Sm}_x\text{FeO}_3$ ceramics have ferroelectric and magnetic properties. These ceramics compounds have been investigated by different possible analysing methods [14, 15, 16]. One of the investigations carried out is the differential scanning calorimetry (DSC), which showed that samarium inserting to BFO T_c temperature moves to lower temperatures, as an example T_c of pure BFO - 1103 K, and the insertion of samarium T_c considerably is reduced (BSF10 – 721 K, BSF15 – 582 K) [15]. $\text{Bi}_{1-x}\text{Dy}_x\text{FeO}_3$ ceramics at lower frequencies up to 1 MHz is dominated by conductivity phenomena [17, 18, 19]. The dielectric measurement results show that the Neel temperature decreases with the dysprosium concentration, say $\text{Bi}_{0.9}\text{Dy}_{0.1}\text{FeO}_3$ Neel temperature is $T_N = 473$ K and BFO $T_N = 638$ K [18].

Aurivillius structure compounds appear to be a promising family for search of new multifunctional materials. A typical representative of this class is $\text{Bi}_4\text{Ti}_3\text{O}_{12}$ (BIT). BIT ceramics have a high Curie temperature value (943 K) [20, 21, 22, 23]. In $\text{Bi}_{4-x}\text{R}_x\text{Ti}_3\text{O}_{12}$,

where $R_x = \text{Pr, Nd, Gd and Dy}$, the rare earth concentration determines the ferroelectric characteristics of the compounds: for small x , they behave as typical ferroelectrics, but all of them tend to become relaxors at $x \geq 0.6$ [24].

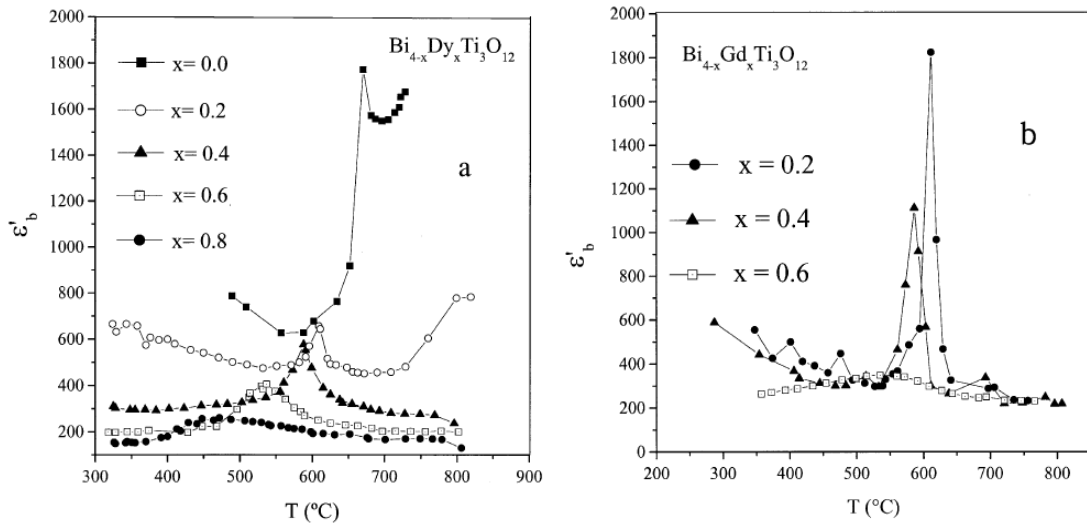


Figure 2.1. Dielectric permittivity versus temperature (a) $\text{Bi}_{4-x}\text{Dy}_x\text{Ti}_3\text{O}_{12}$, (b) $\text{Bi}_{4-x}\text{Gd}_x\text{Ti}_3\text{O}_{12}$: $x = 0.2, 0.4, 0.6, 0.8$ in both cases.

$\text{Ba}_2\text{NdFeNb}_4\text{O}_{15}$, $\text{Ba}_2\text{NdFeNb}_{4-x}\text{Ta}_x\text{O}_{15}$ ceramics belong to the tetragonal tungsten bronze (TTB) structural family, which has attracted much attention in recent years. $\text{Ba}_2\text{NdFeNb}_4\text{O}_{15}$ ($\text{Ln} = \text{La, Pr, Nd, Sm, Eu, Gd}$) family of ceramics is known to have a variety of interesting properties. Compounds with neodymium, samarium and europium are ferroelectrics, while ceramics with praseodymium and gadolinium exhibit relaxor properties [25, 26]. Moreover, Pr, Nd, Sm, Eu, Gd samples exhibit at room temperature magnetic hysteresis loops [25]. Pure $\text{Ba}_2\text{NdFeNb}_4\text{O}_{15}$ compound exhibits an anomalous behaviour of the dielectric permittivity associated with ferroelectric phase transition, which is accompanied by unusually wide thermal hysteresis. On cooling dielectric permittivity peaks strongly move to the lower temperatures. $\text{Ba}_{6-2x}\text{Eu}_{2x}\text{Fe}_{1+x}\text{Nb}_{9-x}\text{O}_{30}$ ($0.6 < x < 1.0$) ceramics evolution is from ferroelectric to relaxor behaviour (when $x \geq 0.9$) [27]. Tetragonal Tungsten Bronze systems of the general formulation $(\text{Ba,Sr})_2\text{Ln}(\text{Fe,Nb,Ta})_4\text{O}_{15}$ allowed for the discovery of the very specific multiferroic composites and of multiple relaxor to ferroelectric crossovers. [28].

3. EXPERIMENTAL METHOD

Measurements of the complex permittivity $\varepsilon^* = \varepsilon' - i\varepsilon''$ were performed in a wide 10 K – 1100 K temperature region and in 20 Hz – 42 GHz frequency range. The LCR-meter HP4284 was used to measure capacitance and loss tangent of samples in 20 Hz — 1 MHz frequency range. In this frequency range the model of the flat dielectric capacitor was used to obtain the complex dielectric permittivity [29]. Measurements of complex transmission coefficients were performed using Agilent 8714ET network analyzer in 1 MHz - 3 GHz frequency range [30]. In this case a multimode capacitor model was used to obtain complex dielectric permittivity. Measurements in 10 GHz – 46 GHz frequency range were performed using a scalar network analyzer R2400 produced by “Elmika” company by placing a thin dielectric rod in the center of a waveguide and monitoring the scalar and transmission coefficients from it [29]. Cylindrically shaped samples were used for measurements. Dimensions of the samples were with different radiuses: in 20 Hz – 1 MHz frequency range, the radius of samples was approximately 10 mm - 3 mm, in 1 MHz – 3 GHz frequency range it was about 1 mm - 0.1 mm, while in 10 GHz – 46 GHz frequency range it was only about 1 mm - 0.01 mm. Silver or platinum paste was used for contacts. An automatic temperature control setup was used to maintain a heating-cooling rate less than 1 K/min.

4. RESULTS AND DISCUSSION

4.1. PMT-PT crystals

Results of broadband dielectric investigations of $0.94\text{PbMg}_{1/3}\text{Ta}_{2/3}\text{O}_3 - 0.06\text{PbTiO}_3$ (0.94PMT-0.06PT or PMT-PT) crystals in wide temperature range from 100 K to 950 K are presented in Fig. 4.1.1. The dielectric properties of investigated PMT-PT crystals are governed at lower temperatures (below 300 K) by polar nanoregions dynamics, and by electrical conductivity at higher temperatures (above 600 K).

The complex electric conductivity σ^* was calculated according to the following relationship: $\sigma^* = i\varepsilon^*\varepsilon_0\omega$, where ω is the angular frequency and ε_0 is the dielectric permittivity of the vacuum. The real part of the complex conductivity was fitted with the Almond-West power law [31]:

$$\sigma(\omega) = \sigma_{DC} + A\omega^s, \quad (1)$$

where: σ_{DC} is the DC conductivity and $A\omega^s$ is the AC conductivity.

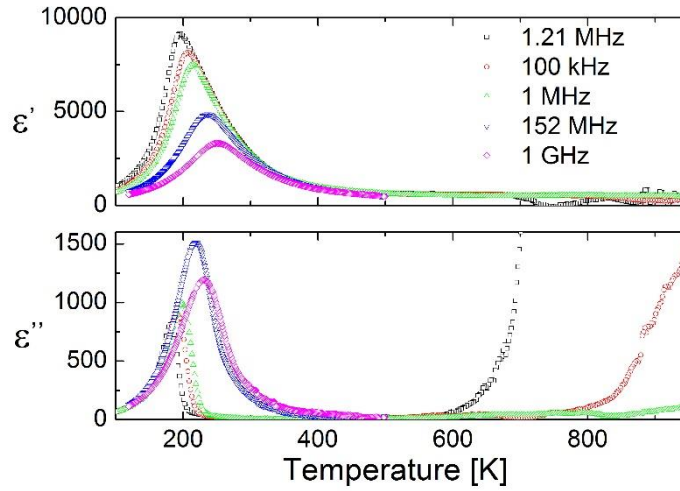


Figure 4.1.1. Temperature dependences of the real (ϵ') and imaginary (ϵ'') parts of complex dielectric permittivity for 0.94PMT-0.06PT crystals at different frequencies.

The $\ln(\sigma_{DC})(1/T)$ dependence has some change in the slope close to 750 K temperature (Fig. 4.1.2.). Therefore, the $\ln(\sigma_{DC})(1/T)$ dependence was fitted with the Arrhenius law $\sigma_{DC} = \sigma_0 \exp(-E_A/kT)$, where σ_0 is the preexponential factor and E_A is the activation energy, separately below and above this temperature. At higher (above 750 K) temperatures the value of activation energy is 0.88 eV, while at lower it is 1.53 eV. The change in conductivity activation energy close to 750 K is related to the change of conductivity mechanism that will be discussed below.

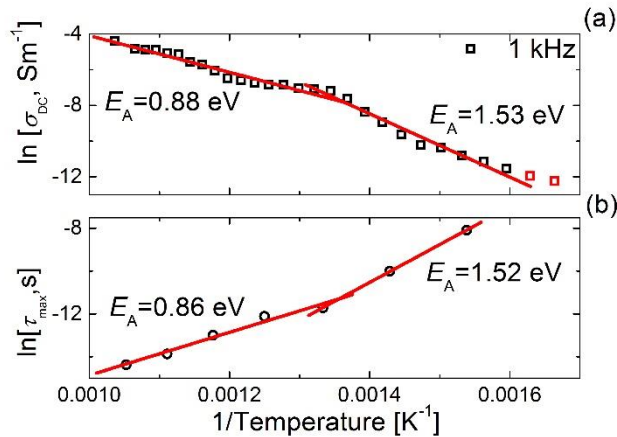


Figure 4.1.2. The $1/T$ dependence of σ_{DC} for 0.94PMT-0.06PT crystals a) and charge transfer mean relaxation time obtained from the electrical modulus spectra for 0.94PMT-0.06PT crystals b).

The electrical conductivity phenomena can also be investigated in terms of the complex electrical modulus $M^* = M' + iM'' = 1/\varepsilon^*$, or

$$M' = \frac{\varepsilon'}{\varepsilon'^2 + \varepsilon''^2},$$

$$M'' = \frac{\varepsilon''}{\varepsilon'^2 + \varepsilon''^2}. \quad (2)$$

The frequency dependences of real (M') and imaginary (M'') parts of complex electric modulus at different temperatures are presented in Fig. 4.1.3. The values of conductivity activation energies indicate that oxygen vacancies should be the most probable electrical charge carrier in 0.94PMT-0.06PT crystals, similarly as in other perovskites [25]. Therefore, the frequency dependences of real (M') and imaginary (M'') parts of complex electric modulus in the 0.94PMT-0.06PT single crystals are related to the oscillation and migration of the oxygen vacancies. At low frequencies, according to Eq. 2, the value of M' is almost zero due to very high losses ε'' (Fig. 4.1.3.) and represents an absence of the restoring energy for the mobile oxygen vacancies.

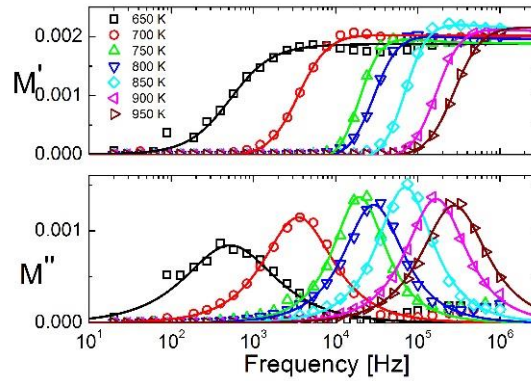


Figure 4.1.3. Frequency dependencies of the real (M') and imaginary (M'') parts of the electrical modulus at different temperatures for 0.94PMT-0.06PT crystals.

The temperature dependence of the conductivity relaxation time is presented in Fig. 4.1.2. b. It demonstrates that the relaxation time of the vacancies is temperature-dependent and the temperature dependence can be described by the Arrhenius law $\tau = \tau_0 \exp(-E_A/kT)$, separately above and below 750 K. The value of activation energy for 0.94PMT-0.06PT single crystals are $E_A = 1.52$ eV below 750 K and $E_A = 0.86$ eV above 750 K. At higher temperatures the values of the activation energy obtained from conductivity relaxation time and DC conductivity are very similar. At the same time at lower temperatures (below 750 K) the values of the activation energies are different, indicating a broad distribution

of conductivity relaxation times (Fig. 4.1.3.). The decreasing in the dc conductivity activation energy at 750 K can be explained by increasing concentration of single ionized vacancies.

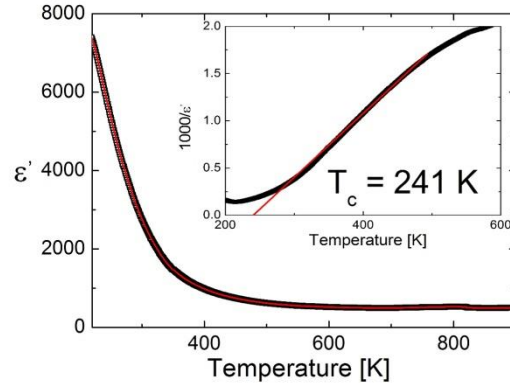


Figure 4.1.4. Temperature dependence of static dielectric permittivity for 0.94PMT-0.06PT crystals with fit according to Eq. 3. Inset shows the temperature dependence of the reciprocal static dielectric permittivity with Curie-Weiss law fit.

No anomaly in the temperature dependence of the static dielectric permittivity was observed in wide temperature range from 213 K to 950 K. The temperature dependence of the static dielectric susceptibility of 0.94PMT-0.06PT single crystals is shown in Fig. 4.1.4. The inset presents the temperature dependence of the reciprocal dielectric permittivity with a linear fit. It is clearly visible that the *Curie-Weiss* fit valid only in some narrow temperature range. According to the SBRF model [32] the static dielectric permittivity follows:

$$\varepsilon' = \frac{\beta(1-q)}{1-\beta J_0(1-q)}, \quad (3)$$

where: $\beta=1/kT$, J_0 is the mean interaction energy and q is the Edwards-Anderson order parameter ($0 \leq q \leq 1$). Where $q = 0$ Eq. 3 becomes a simple Curie-Weiss law. The static dielectric permittivity was successfully described by SBRF model Eq. 3 in wide temperature range (Fig. 4.1.4.). According to Eq. 3 the static dielectric permittivity not have the maximum at $T > 0$, when the Edwards-Anderson parameter decreases with the temperature. In other words, the static dielectric permittivity does not decrease on cooling.

4.2. $\text{Bi}_{1-x}\text{Sm}_x\text{FeO}_3$ ceramics

Results of broadband dielectric investigations of samarium doped bismuth ferrite ceramics were investigated in wide temperature range (20 – 800 K). Results of the dielectric measurements are presented in Fig. 4.2.1. At lower frequencies and higher temperatures (above 400 K) the increase in both real and imaginary parts of the complex dielectric permittivity with temperature is caused by electrical conductivity effects. At temperatures higher than 400 K dielectric anomalies are caused by Maxwell-Wagner polarization [10].

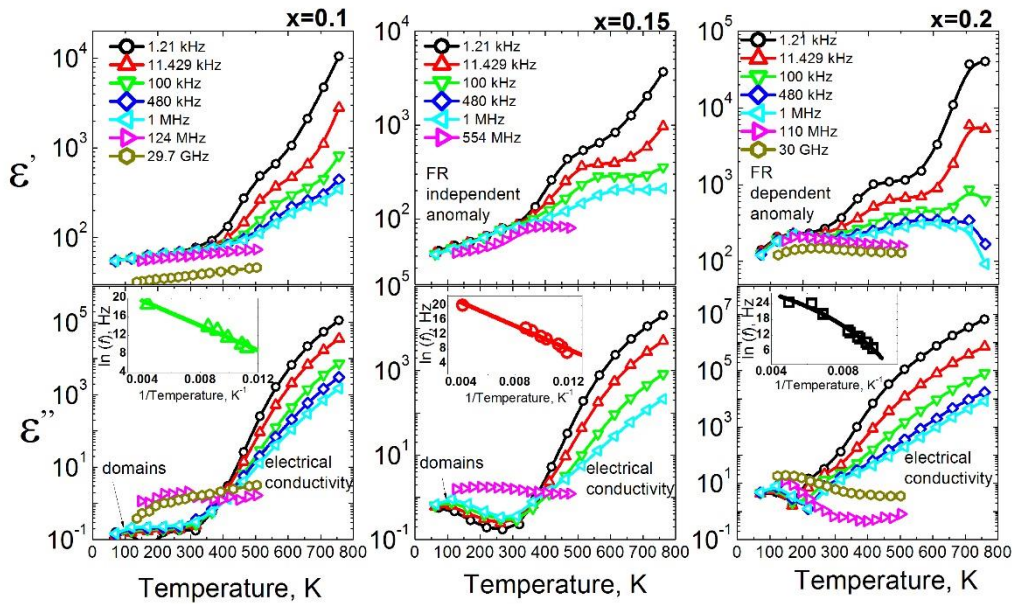


Figure 4.2.1. Temperature dependence of the real (ϵ') and imaginary (ϵ'') parts of complex dielectric permittivity of $\text{Bi}_{1-x}\text{Sm}_x\text{FeO}_3$ ceramics at different frequencies. The inset shows temperature dependence the maximum of imaginary part versus frequency.

At low temperatures (below 200 K) the maximum position of the imaginary part of the complex dielectric permittivity is frequency-dependent (inset in Fig. 4.2.1.). The dependence fits the Arrhenius law $\nu = \nu_0 \exp(-U_{VF}/T)$. The values of parameters that fit Arrhenius law are $\nu_0 = 5.8 \times 10^{10}$ Hz and $U_{VF} = 1335$ K where $x = 0.1$; $\nu_0 = 8.0 \times 10^{11}$ Hz and $U_{VF} = 1618$ K, where $x = 0.15$. The dependence fits the Vogel-Fulcher law $\nu = \nu_0 \exp(-U_{VF}/[T - T_f])$. Obtained parameters are $T_f = 57.8$ K, $\nu_0 = 9.9 \times 10^{14}$ Hz, and $U_{VF} = 1271$ K where $x = 0.2$. For compounds $x = 0.1$ and $x = 0.15$ where the ferroelectric order does not

disappear [33] the dielectric dispersion at very low temperatures should be caused by ferroelectric domains dynamics. However, at $x = 0.2$ no ferroelectric order was detected by piezoelectric force microscopy [33] and ferroelectric domains dynamics cannot be originated from dielectric dispersion.

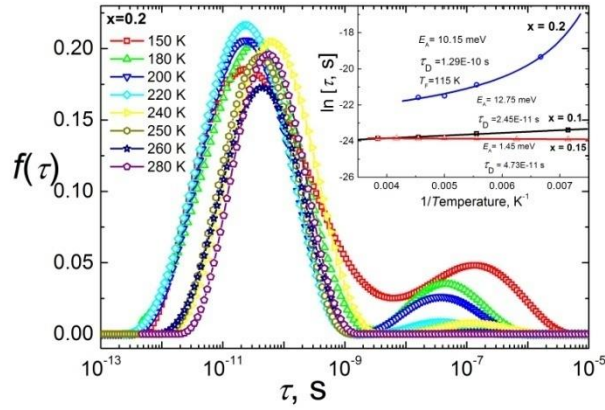


Figure 4.2.2. Distribution of relaxation times $f(\tau)$ of $\text{Bi}_{0.8}\text{Sm}_{0.2}\text{FeO}_3$ ceramics calculated at different temperatures. The inset shows temperature dependence of maximum relaxation time for $\text{Bi}_{1-x}\text{Sm}_x\text{FeO}_3$ ceramics.

The Tikhonov regularization method was used. This method and calculation technique is described in details elsewhere [34]. The distributions of relaxation times are presented in Fig. 4.2.2. At low temperatures (below 230 K) the longest relaxation times (0.1 of maximum $f(\tau)$) was chosen for definition) were obtained from the distribution function and fitted with the Vogel-Fulcher law (see inset Fig. 4.2.2.) $\tau(T) = \tau_D \exp(E_B/k(T - T_f))$. Obtained values are $E_B = 10.15$ meV, $\tau_D = 1.29 \times 10^{-10}$ s and $T_f = 115$ K. The values of parameters that fit Arrhenius law are $E_A = 12.75$ meV, $\tau_D = 4.73 \times 10^{-11}$ s where $x = 0.1$ and $E_A = 1.45$ meV, $\tau_D = 2.45 \times 10^{-11}$ s where $x = 0.15$. The frequency-dependent maximum of complex dielectric permittivity in all frequency range, broad dielectric dispersion and two maxima in distribution of relaxation times are typical for ferroelectric relaxors [35]. In samarium doped bismuth ferrite the ferroelectric phase transition temperature decreases with samarium concentration and finally no ferroelectric order is observed at $x = 0.2$. At lower temperatures the dielectric properties of ferroelectric samarium doped bismuth ferrite are governed by ferroelectric domains dynamics. Ceramics with $x = 0.2$ exhibit the relaxor-like behaviour.

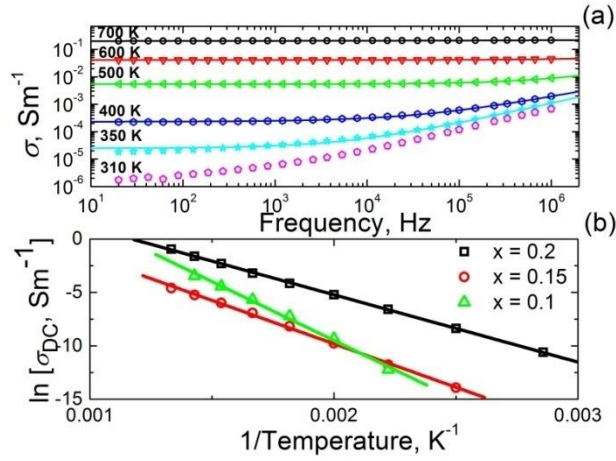


Figure 4.2.3. (a) Frequency dependencies of DC conductivity at different temperatures for $\text{Bi}_{0.8}\text{Sm}_{0.2}\text{FeO}_3$ ceramics. (b) The $1/T$ dependence of σ_{DC} for $\text{Bi}_{1-x}\text{Sm}_x\text{FeO}_3$ ceramics.

At higher temperatures (above 400 K) the electrical conductivity dominates in the properties of ceramics. Fig. 4.2.3. (a) shows the frequency dependence of conductivity at different temperatures for $\text{Bi}_{1-x}\text{Sm}_x\text{FeO}_3$ ceramics (with $x = 0.2$) (Eq. 1). With increasing Sm concentration the DC conductivity can be determined at lower temperatures (in the frequency range of our measurements), for example when $x = 0.2$ the DC conductivity can be determined even at $T=350$ K. The values of DC conductivity for ceramics with $x = 0.1$ and $x = 0.15$ are similar, while for ceramics $x = 0.2$ it is substantially higher. From obtained values of σ_{DC} at different temperatures activation energy (E_A) and pre-exponential factor σ_0 of the conductivity according to the Arrhenius law $\sigma_{\text{DC}} = \sigma_0 \exp(-E_A/kT)$ can be calculated (Fig. 4.2.3. (b)). The value of activation energy for $\text{Bi}_{1-x}\text{Sm}_x\text{FeO}_3$ ceramics is $E_A = 0.95$ eV and $\sigma_0 = 278662 \text{ Sm}^{-1}$ (where $x = 0.1$); $E_A = 0.70$ eV and $\sigma_0 = 636 \text{ Sm}^{-1}$ (where $x = 0.15$); $E_A = 0.54$ eV and $\sigma_0 = 1605 \text{ Sm}^{-1}$ (where $x = 0.2$). In $\text{Bi}_{1-x}\text{Sm}_x\text{FeO}_3$ ceramics the DC conductivity increases and activation energy decreases with samarium concentration, especially at higher samarium concentrations.

4.3. $\text{Bi}_{1-x}\text{Dy}_x\text{FeO}_3$ ceramics

$\text{Bi}_{1-x}\text{Dy}_x\text{FeO}_3$ ($x = 0.2, x = 1.5, x = 0.1$) dielectric and electrical conductivity properties have not been investigated in detail so far. Dielectric and electric investigations in the scope of this research were performed at frequencies 20 Hz - 1 MHz in 25 K - 1050 K temperature range. The dielectric permittivity and the impedance variation with

temperature were analysed for $\text{Bi}_{1-x}\text{Dy}_x\text{FeO}_3$, where $x = 0.1, x = 0.15, x = 0.2$ ceramics (Fig. 4.3.1).

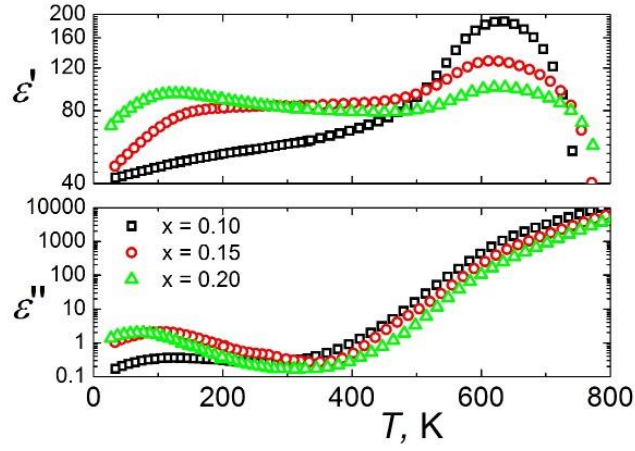


Figure 4.3.1. Temperature dependence of the real (ϵ') and imaginary (ϵ'') parts of the complex dielectric permittivity of $\text{Bi}_{1-x}\text{Dy}_x\text{FeO}_3$ with $x = 0.1, x = 0.15$ and $x = 0.2$ at 1 MHz frequencies.

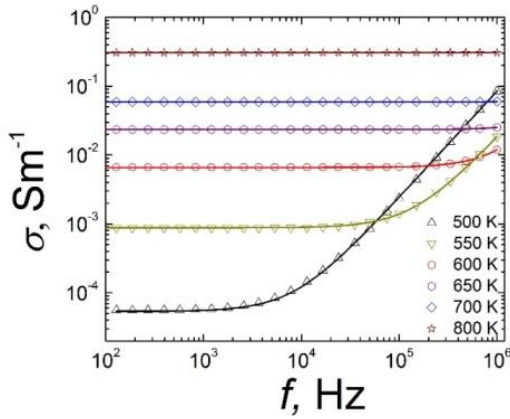


Figure 4.3.2. Frequency dependencies of DC conductivity at different temperatures for $\text{Bi}_{0.8}\text{Dy}_{0.2}\text{FeO}_3$ ceramics.

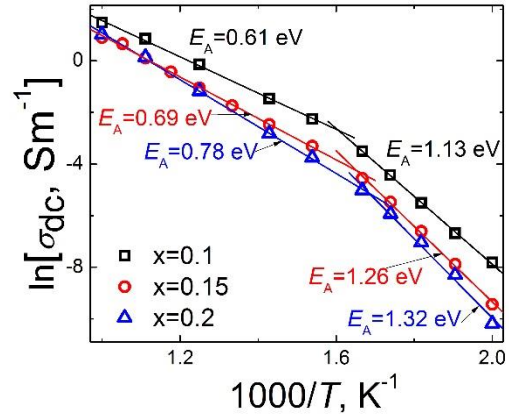


Figure 4.3.3. The $1/T$ dependence of σ_{DC} for $\text{Bi}_{1-x}\text{Dy}_x\text{FeO}_3$ with $x=0.1, 0.15$ and 0.2 .

Above 500 K, results in terms of the conductivity will be discussed [Fig. 4.3.2.]. At low frequencies the conductivity phenomena dominate in the dielectric spectra. The carrier's relaxation time increase with temperature, so that the complex resistivity dispersion is observed at higher frequencies [17]. The conductivity also increases with dysprosium concentration. The electric conductivity σ was calculated according to Eq. 1. From the obtained values of σ_{DC} at different temperatures, the activation energy E_A and pre-exponential factor σ_0 according to the Arrhenius law $\sigma_{\text{DC}} = \sigma_0 \exp(-E_A/kT)$ can be calculated (Fig. 4.3.3). The value of activation energy for $\text{Bi}_{1-x}\text{Dy}_x\text{FeO}_3$ when $x = 0.1$ are

$E_A = 1.13$ eV below 625 K and $E_A = 0.61$ eV above 625 K, when $x = 0.15$ are $E_A = 1.26$ eV below 605 K and $E_A = 0.69$ eV above 605 K, when $x = 0.2$ are $E_A = 1.32$ eV below 590 K and $E_A = 0.78$ eV above 590 K. Thus the conductivity activation energy increases with dysprosium concentration. Taking into account the values of activation energies obtained above, oxygen vacancies should be the most probable electrical charge carrier [36].

4.4. $\text{Bi}_{4-x}\text{Gd}_x\text{Ti}_3\text{O}_{12}$ ceramics

The present work is aimed at dielectric investigation of undoped and gadolinium-substituted Aurivillius-structure bismuth titanates $\text{Bi}_4\text{Ti}_3\text{O}_{12}$ (BIT) and $\text{Bi}_{4-x}\text{Gd}_x\text{Ti}_3\text{O}_{12}$ (BGT). The measurements were performed as a function of both frequency and temperature in the frequency range of 20 Hz – 1 MHz and in the temperature range of 30 – 1100 K.

The results of dielectric measurements are presented in Figs. 4.4.1., 4.4.2. A dielectric anomaly is observed in $\text{Bi}_4\text{Ti}_3\text{O}_{12}$ ceramics at low temperatures (Figs. 4.4.1. (a), 4.4.2. (a)). At low temperatures the position of maximum of the real part of complex dielectric permittivity is frequency-dependent (Fig. 4.4.1. (a)). On the other hand, the temperature dependence of imaginary part of complex dielectric permittivity exhibits two overlapped and frequency-dependent maxima (Fig. 4.4.2. (a)). Both these maxima shift to higher temperatures with the increase of the frequency. Such a behaviour of complex dielectric permittivity can be attributed to ferroelectric domain dynamic [37] or dipolar glass type behaviour [38] or ferroelectric relaxor behaviour [1]. At higher temperatures (above 400 K) the phenomena of electrical conductivity are observed in the dielectric spectra of BGT ceramics (Figs. 4.4.1. (b) and 4.4.2. (b)). The anomaly of electrical conductivity at 940 K in BIT ceramics is related to the ferroelectric phase transition reported in [20, 22]. Instead, temperature [Fig. 4.4.3.] dependencies of the imaginary part dielectric permittivity maxima positions were determined, which both for $\text{Bi}_{4-x}\text{Gd}_x\text{Ti}_3\text{O}_{12}$ ceramics, with $x = 0$ and $x = 1.5$, follow the Vogel-Fulcher equation $f = f_0 \exp(E_A/(k[T - T_0]))$, indicating a considerable shift of T_0 with increasing x . The validity of this relationship does not clearly distinguish between ferroelectric domain dynamics of dipole glass or ferroelectric relaxor behaviour. It is unlikely that the disorder typical of ferroelectric relaxor or dipolar glass would disappear by introducing impurities (in this

case gadolinium), so pure BIT dielectric dispersion at low temperatures is also caused by the dynamics of ferroelectric domains.

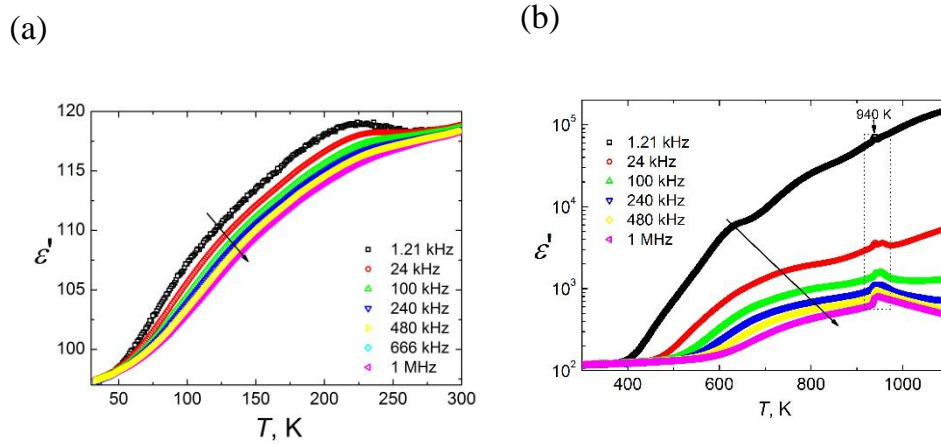


Figure 4.4.1. Temperature dependence of the real (ϵ') part of the complex dielectric permittivity of $\text{Bi}_4\text{Ti}_3\text{O}_{12}$ at different frequencies (a) at lower temperatures, (b) at higher temperatures.

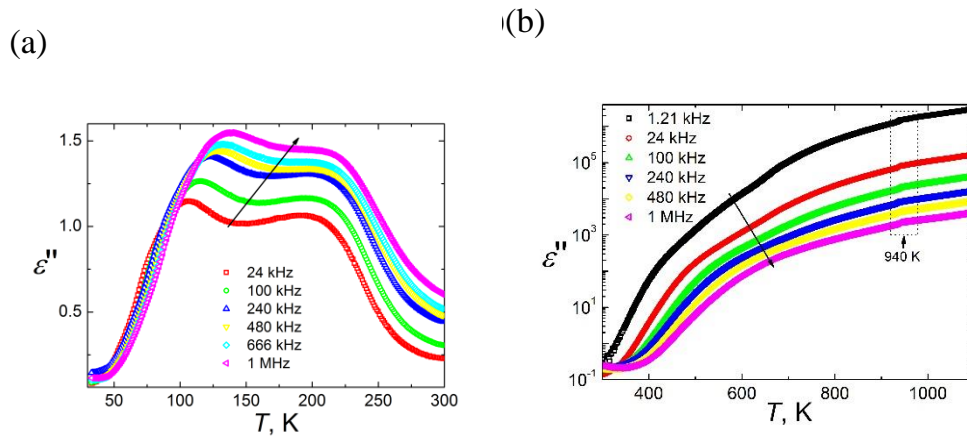


Figure 4.4.2. Temperature dependence of the imaginary (ϵ'') part of the complex dielectric permittivity of $\text{Bi}_4\text{Ti}_3\text{O}_{12}$ at different frequencies (a) at lower temperatures, (b) at higher temperatures.

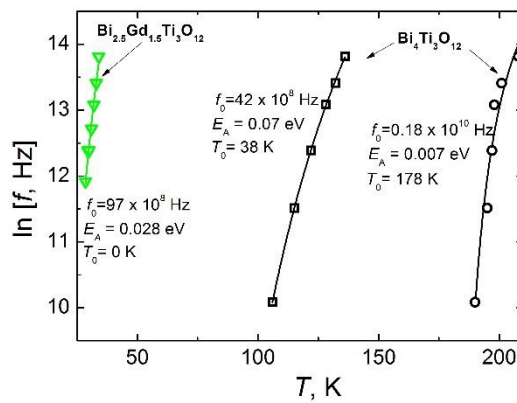


Figure 4.4.3. Temperature dependencies of the imaginary part of complex dielectric permittivity of $\text{Bi}_{4-x}\text{Gd}_x\text{Ti}_3\text{O}_{12}$ ceramics with $x = 0$ and $x = 1.5$, fitted with Vogel-Fulcher equation.

At higher temperatures (above 500K) the low-frequency permittivity is dominated by conductivity effects. To distinguish the grain conductivity from intergrain conductivity, specific resistance was calculated according to the following formulae:

$$\rho^* = \frac{1}{\sigma^*(\omega)} = \rho'(\omega) - i\rho''(\omega) = \frac{\varepsilon'^2 - i\varepsilon''^2}{\varepsilon_0\omega(\varepsilon'^2 + \varepsilon''^2)}, \quad (4)$$

where: $\omega=2\pi f$, f is the measurement frequency.

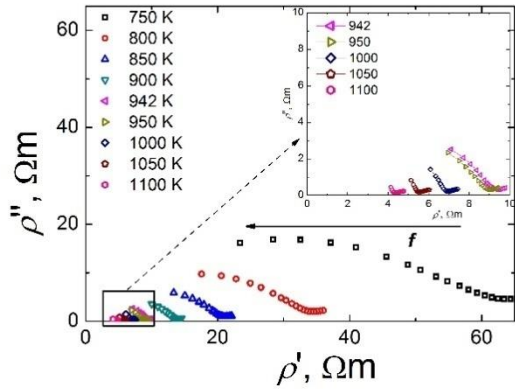


Figure 4.4.4. Nyquist diagram for specific resistance of $\text{Bi}_4\text{Ti}_3\text{O}_{12}$.

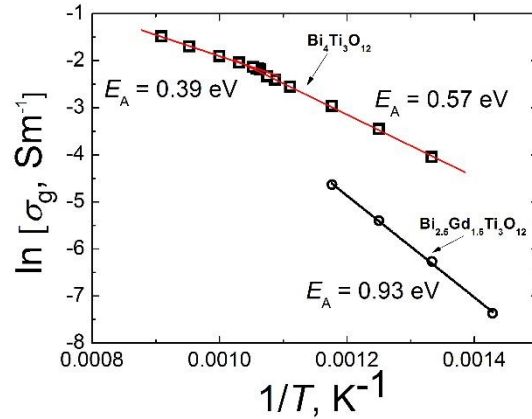


Figure 4.4.5. Electrical conductivity of the grains in $\text{Bi}_4\text{Ti}_3\text{O}_{12}$ and $\text{Bi}_{2.5}\text{Gd}_{1.5}\text{Ti}_3\text{O}_{12}$ ceramics.

The results are presented in Fig. 4.4.4. One can clearly see that there are two semicircles, which can be attributed to the grain, intergrain conductivity and blocking contacts effect. The semicircle at higher frequencies (and lower values of resistance) are usually caused by the volume conductivity of ceramic, while the higher value of ρ^* accounts for intergrain processes and can be also influenced by blocking contacts. From the left semicircle, the grain specific resistance ρ_{gr} at different temperature was calculated. The bulk activation energy of the grains E_A was calculated from the temperature dependence of $\sigma_g=1/\rho_g$ according to the Arrhenius law. The fracture in temperature dependence of the grains conductivity close to 940 K is visible in figure 4.4.5. Therefore, the conductivity activation energy values are different below and above this temperature. Above 940 K the activation energy is equal to 0.39 eV. Activation energy in bulk of $\text{Bi}_{2.5}\text{Gd}_{1.5}\text{Ti}_3\text{O}_{12}$ ceramic estimated from the specific resistance measurements was found to be $E_A=0.93$ eV. The results are of primary importance for understanding the peculiarities of conductivity behaviour in layered Aurivillius-type compounds.

4.5. $\text{Ba}_{6-2x}\text{Nd}_{2x}\text{Fe}_{1+x}\text{Nb}_{9-x}\text{O}_{30}$ ceramics

This work presents broadband dielectric spectroscopy results of a new $\text{Ba}_{6-2x}\text{RE}_{2x}\text{Fe}_{1+x}\text{Nb}_{9-x}\text{O}_{30}$ (RE = Nd) ($x=0.6, 0.8, 1$) (BNFN) system. The investigations were carried out for samples $x = 0.6, 0.8$ and 1 . Dielectric measurements were performed in 30 K— 450 K temperature region and 20 Hz – 46 GHz frequency range.

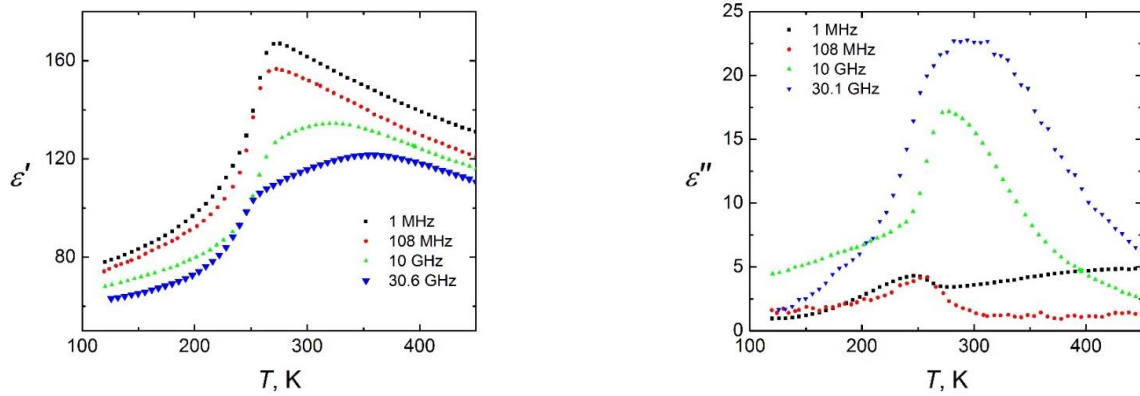


Figure 4.5.1. Temperature dependence of the real (ϵ') and imaginary (ϵ'') parts of the complex dielectric permittivity of $\text{Ba}_2\text{NdFeNb}_4\text{O}_{15}$ at different frequencies.

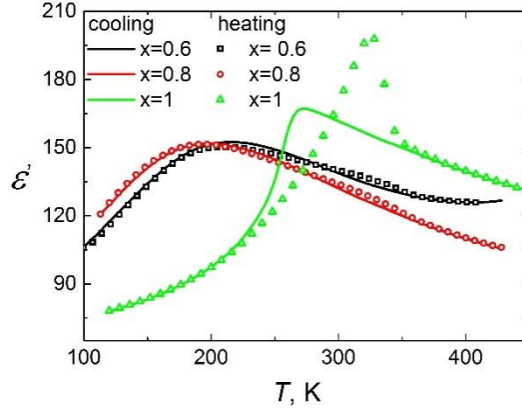


Figure 4.5.2. Temperature dependence of the dielectric permittivity for $\text{Ba}_{6-2x}\text{Nd}_{2x}\text{Fe}_{1+x}\text{Nb}_{9-x}\text{O}_{30}$ ceramics with different x on heating (symbols) and cooling (lines) at 1 MHz frequency.

For $\text{Ba}_2\text{NdFeNb}_4\text{O}_{15}$ ceramics dielectric measurement results are presented in Fig. 4.5.1. For $\text{Ba}_{6-2x}\text{Nd}_{2x}\text{Fe}_{1+x}\text{Nb}_{9-x}\text{O}_{30}$ ceramics the temperature dependence of the dielectric permittivity at 1 MHz frequency is presented in Fig. Fig. 4.5.2. The huge dielectric anomaly is observed in all ceramics, which position is strongly dependent from x . Moreover, in $\text{Ba}_2\text{NdFeNb}_4\text{O}_{15}$ compound the strong hysteresis between heating and cooling cycle close to the dielectric anomaly temperature is observed, the mismatch

between the dielectric permittivity maximum temperature in heating and cooling cycles is higher as 50 K temperature (Fig. 4.5.2). The position of the dielectric permittivity maximum is frequency independent for $x=1$. The hysteresis loop becomes smaller for compounds with Nd and remains very low or completely disappears for $x=0.8$.

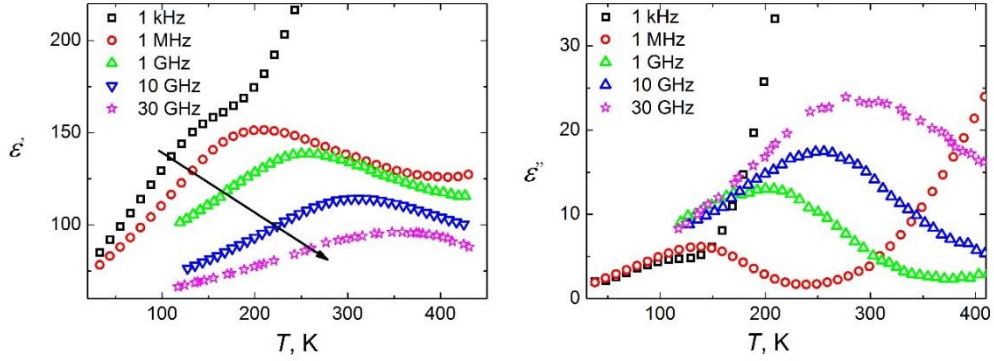


Figure 4.5.3. Temperature dependence of the real (ϵ') and imaginary (ϵ'') parts of dielectric permittivity for $\text{Ba}_{6-2x}\text{Nd}_{2x}\text{Fe}_{1+x}\text{Nb}_{9-x}\text{O}_{30}$ ceramics when $x = 0.6$ at different frequencies.

The temperature dependence of the real and imaginary parts of dielectric permittivity of BNFN ceramics when $x = 0.6$ is presented in Fig. 4.5.3. An anomaly of the dielectric permittivity which is typical of ferroelectric relaxors was observed. In this case, conductivity starts influencing low frequency dielectric spectra above 120 K. Looking into BNFN ceramics in Fig. 4.5.1. and Fig. 4.5.3. it can be said that with decreasing Nd concentration their dielectric behaviour changes from ferroelectric to relaxor.

In order to elucidate such unusual temperature dielectric response of $\text{Ba}_{6-2x}\text{Nd}_{2x}\text{Fe}_{1+x}\text{Nb}_{9-x}\text{O}_{30}$ ($x = 0.6$) ceramics frequency dependencies of the dielectric permittivity in a wide temperature range from 180 K to 300 K were examined covering both dielectric anomalies. Characteristic frequency dependencies of the real and the imaginary parts of complex dielectric permittivity at selected temperatures are shown in Fig.4.5.4. The dielectric spectra look like symmetric therefore for fitting the Cole-Cole equation was used with electrical conductivity term (Eq. 5). Solid lines represent the best fit of Cole – Cole equation.

$$\epsilon^* = \epsilon' - i\epsilon'' = \epsilon_\infty + \frac{\Delta\epsilon}{1 + (i\omega\tau)^{1-\alpha}} - \frac{i\sigma^*}{\epsilon_0\omega} \quad (5)$$

where: ε_∞ – dielectric permittivity when $\omega \rightarrow \infty$; $\Delta\varepsilon$ – the strength of relaxator; τ – the mean relaxation time; α – the width of Cole-Cole distribution of relaxation time; σ^* – the frequency dependent conductivity; ε_0 – the vacuum permittivity, and σ is the conductivity, reflecting the input of conductivity process.

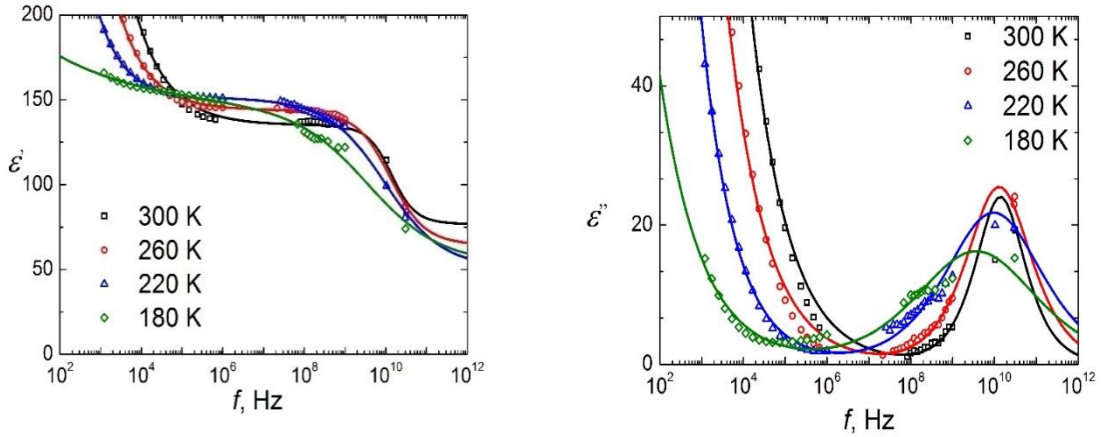


Figure 4.5.4. Frequency dependence of the real (ε') and imaginary (ε'') parts of dielectric permittivity for $\text{Ba}_{6-2x}\text{Nd}_{2x}\text{Fe}_{1+x}\text{Nb}_{9-x}\text{O}_{30}$ ceramics when $x = 0.6$ at different temperatures.

It is clearly observed from Fig. 4.5.4. that it is impossible to describe the results only with Cole-Cole equation, so in order to adjust the results relaxation time distribution function was used (Eq. 6). General approach had to be used for determination of the real and continuous distribution function of relaxation times $f(\tau)$ by solving Fredholm integral equation [34]:

$$\varepsilon^*(\nu) = \varepsilon_\infty + \Delta\varepsilon \int_{-\infty}^{\infty} \frac{f(\tau) d \ln \tau}{1 + i\omega\tau} \quad (6)$$

The distribution of relaxation times $f(\tau)$ of TTB ceramics when $x = 0.6$ calculated at different temperatures is shown in Fig. 4.5.5. On cooling the distributions of relaxations times becomes broader and more asymmetric. Fig. 4.5.6 shows the temperature dependence of characteristic (longest, most probable and Cole-Cole mean) relaxation times for both investigated TTB ceramics. The most probable and longest ((level 0.1 of the maximum $f(\tau)$) was chosen for definition of the distributions limits) relaxation times were obtained from the distribution function (Fig. 4.5.5.) and fitted with the Vogel-Fulcher law $\tau(T) = \tau_0 \exp(E/(k(T-T_f)))$. Solid lines represents a fit of the Vogel-Fulcher law. The

activation energy increases with Nd concentration, while the freezing temperature decreases.

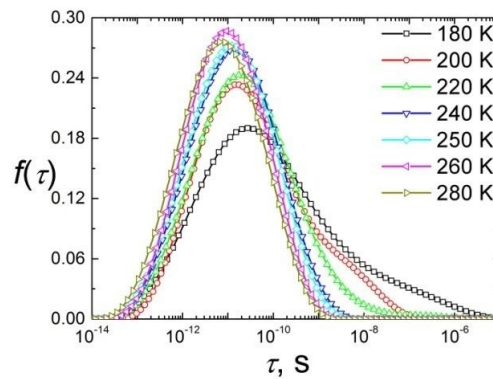


Figure 4.5.5. Distribution of relaxation times $f(\tau)$ of $\text{Ba}_{4.8}\text{Nd}_{1.2}\text{Fe}_{1.6}\text{Nb}_{8.4}\text{O}_{30}$ calculated at different temperatures.

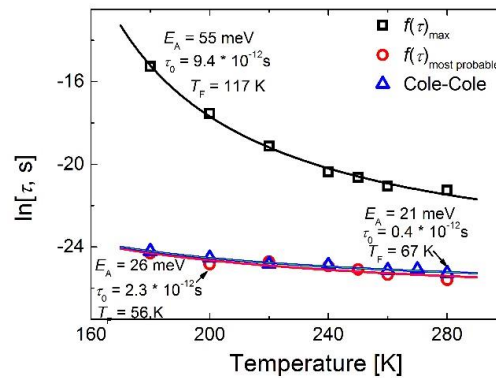


Figure 4.5.6. Temperature dependences of the mean relaxation times (Cole-Cole), and the most probable and longest relaxation times of $f(\tau)$ curves of $\text{Ba}_{6-2x}\text{Nd}_{2x}\text{Fe}_{1+x}\text{Nb}_{9-x}\text{O}_{30}$ ceramic when $x = 0.6$. Solid lines represent a fit of the Vogel-Fulcher law.

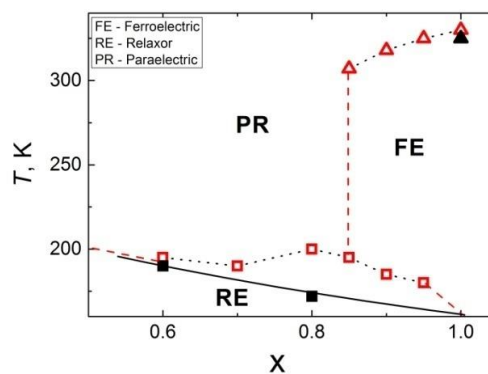


Figure 4.5.7. $\text{Ba}_{6-2x}\text{Nd}_{2x}\text{Fe}_{1+x}\text{Nb}_{9-x}\text{O}_{30}$ ceramic phase diagram. The solid points are obtained experimentally and the hollow points are taken from the reference [25]. Triangular points show the phase transition from paraelectric to ferroelectric. Squares points show maxima of real part ϵ' of relaxor at 100 kHz frequencies. The lines are guide for eye.

Fig. 4.5.7. shows $\text{Ba}_{6-2x}\text{Nd}_{2x}\text{Fe}_{1+x}\text{Nb}_{9-x}\text{O}_{30}$ ceramics phase diagram at 100 kHz frequencies. BNFN ceramic has both ferroelectric and relaxor properties when x is between 0.85 and 0.95 [25, 39]. Typical relaxor behaviour is observed in BNFN ceramics when $x < 0.85$.

4.6. $\text{Ba}_2\text{NdFeNb}_{4-x}\text{Ta}_x\text{O}_{15}$ ceramics

Dielectric response of $\text{Ba}_2\text{NdFeNb}_{4-x}\text{Ta}_x\text{O}_{15}$ ($x = 0.3, 0.6$ and 2) solid solutions with Tetragonal Tungsten Bronze structure was investigated by means of broadband dielectric spectroscopy in the frequency range from 20 Hz to 37 GHz.

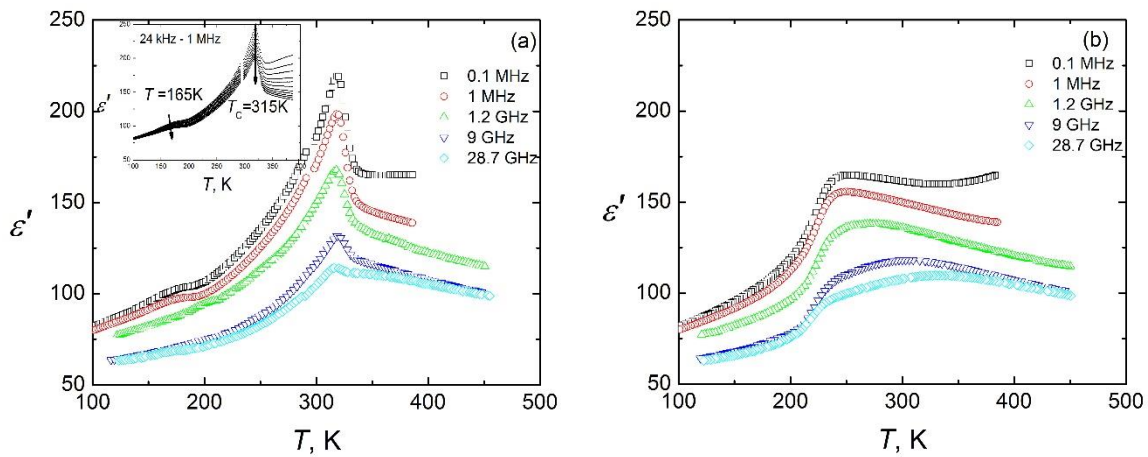


Figure 4.6.1. Temperature dependencies of the real (ϵ') part of complex dielectric permittivity of $\text{Ba}_2\text{NdFeNb}_{3.7}\text{Ta}_{0.3}\text{O}_{15}$ ceramic at different frequencies on heating (a) and cooling (b).

Investigations of dielectric properties of $\text{Ba}_2\text{NdFeNb}_{3.7}\text{Ta}_{0.3}\text{O}_{15}$ ceramics revealed two completely different responses to heating and cooling. Corresponding temperature dependencies of the real part of complex dielectric permittivity at selected frequencies are shown in Fig. 4.6.1. On heating two dielectric anomalies can be distinguished – a diffuse one in the 150 K – 200 K temperature range and well expressed peaks at 315 K. The latter anomaly of ϵ' has a characteristic form similar to that observed in pure $\text{Ba}_2\text{NdFeNb}_4\text{O}_{15}$ ceramics [26], the frequency-independent dielectric anomaly at 325 K has been associated with the ferroelectric phase transition. 10 K lower ferroelectric phase transition temperature in $\text{Ba}_2\text{NdFeNb}_{3.7}\text{Ta}_{0.3}\text{O}_{15}$ ceramics is most likely related to the introduction of Ta^{5+} cations, which also causes the appearance of additional low temperature dielectric

dispersion region. On the following cooling run of dielectric measurements, a huge shift of permittivity maxima to lower temperatures (248 K) is observed. This lowering is accompanied by a complete change of the form of ϵ' temperature dependencies, which now obtain a diffuse shape, more characteristic to relaxors than to ferroelectric phase transition.

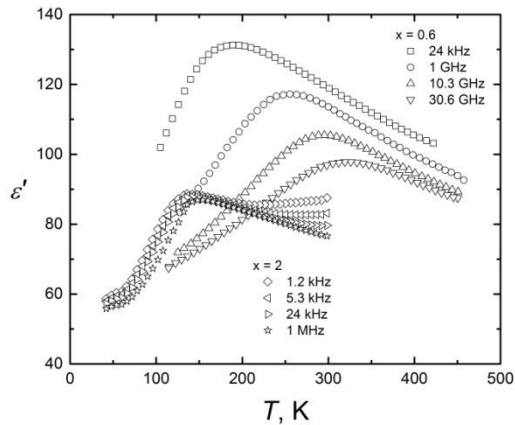


Figure 4.6.2. Temperature dependencies of the real (ϵ') part of complex dielectric permittivity of $\text{Ba}_2\text{NdFeNb}_{4-x}\text{Ta}_x\text{O}_{15}$ ceramics with $x = 0.6$ and $x = 2$.

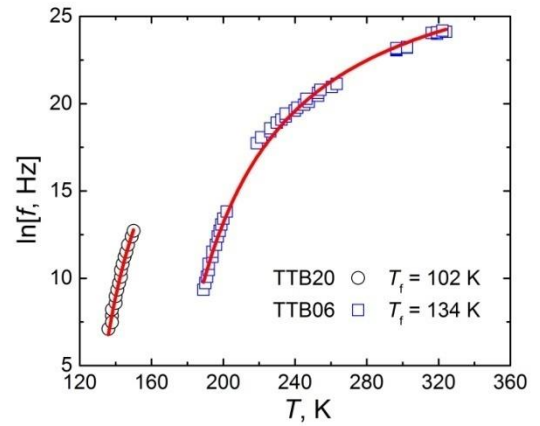


Figure 4.6.3. Temperature dependencies of dielectric permittivity maxima positions for $\text{Ba}_2\text{NdFeNb}_{3.4}\text{Ta}_{0.6}\text{O}_{15}$ ($x = 0.6$) and $\text{Ba}_2\text{NdFeNb}_2\text{Ta}_2\text{O}_{15}$ ($x = 2$) ceramics, fitted with Vogel-Fulcher equation.

Investigations of $\text{Ba}_2\text{NdFeNb}_{3.4}\text{Ta}_{0.6}\text{O}_{15}$ ($x = 0.6$) sample with a higher concentration of tantalum showed that the dielectric response completely changes its shape. Unlike for the previous sample ($x = 0.3$), here no heating – cooling hysteresis is observed. Also, no permittivity maxima or dispersion were found, which could be associated with ferroelectric phase transition. Variation of ϵ' and ϵ'' with temperature and frequency shows a "classical" example of a ferroelectric relaxor dielectric response [1]. Analysis of frequency dependencies of complex dielectric permittivity in a 20 Hz - 36 GHz range at 300 K - 150 K temperatures revealed one broad dielectric relaxation process, which means relaxation time follows the Vogel-Fulcher law. Further increase of Ta^{5+} content in $\text{Ba}_2\text{NdFeNb}_{4-x}\text{Ta}_x\text{O}_{15}$ structure shifts the dielectric dispersion region towards lower temperatures (Fig. 4.6.2.). Again, observed temperature dependencies of the real and the imaginary parts of the dielectric permittivity have a typical ferroelectric relaxor form. The experimental setup of this research was limited to 1 MHz at low temperatures, therefore, we were unable to define relaxation parameters for this process. Instead, temperature

dependencies of dielectric permittivity maxima positions were determined, which both for $\text{Ba}_2\text{NdFeNb}_{3.4}\text{Ta}_{0.6}\text{O}_{15}$ ($x = 0.6$) and $\text{Ba}_2\text{NdFeNb}_2\text{Ta}_2\text{O}_{15}$ ($x = 2$) ceramics follow Vogel-Fulcher equation (Fig. 4.6.3.), indicating a considerable shift of T_f with increasing x .

Dielectric response of $\text{Ba}_2\text{NdFeNb}_{3.7}\text{Ta}_{0.3}\text{O}_{15}$ solid solution exhibits features of ferroelectric and ferroelectric relaxor states. Similar possible coexistence was reported for $\text{Ba}_2\text{Pr}_x\text{Nd}_{1-x}\text{FeNb}_4\text{O}_{15}$ compounds [26], where relaxor properties were induced by rare earth ion substitutions at A2 sites. Introduction of Ta^{5+} cations within the octahedral framework also causes the appearance of relaxor like dielectric dispersion region in these TTBs and shifts the ferroelectric phase transition to slightly lower temperatures. Despite these differences, cationic substitutions inside square channels and octahedral framework of these TTBs yield qualitatively to the same kind of dielectric behavior - ferroelectric to relaxor crossover. Since Ta^{5+} replaces ferroelectrically active Nb^{5+} cations and introduces additional disorder in these systems, it enables relaxor state expression in $\text{Ba}_2\text{NdFeNb}_{4-x}\text{Ta}_x\text{O}_{15}$ solid solutions by suppressing ferroelectric state. With increasing Ta^{5+} concentration the complete vanishing of ferroelectric state was observed together with considerable lowering of relaxor dispersion region temperatures.

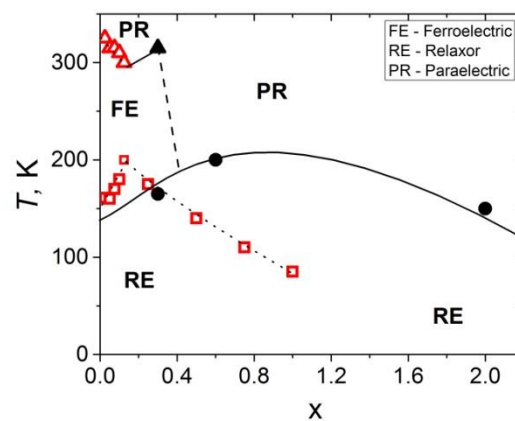


Figure 4.6.4. $\text{Ba}_2\text{NdFeNb}_{4-x}\text{Ta}_x\text{O}_{15}$ ceramic phase diagram. The solid points are obtained experimentally and the hollow points are taken from the reference [25]. Triangular points show the phase transition from paraelectric to ferroelectric. Squares points show maxima of real part ϵ' of relaxor at 1 MHz frequencies. The lines are guide for eye.

Fig. 4.6.4. shows $\text{Ba}_2\text{NdFeNb}_{4-x}\text{Ta}_x\text{O}_{15}$ ceramics phase diagram at 1 MHz frequencies. $\text{Ba}_2\text{NdFeNb}_{4-x}\text{Ta}_x\text{O}_{15}$ ceramic has both ferroelectric and relaxor properties

when x is between 0 and 0.3 [25, 39]. Typical relaxor behaviour is observed in $\text{Ba}_2\text{NdFeNb}_{4-x}\text{Ta}_x\text{O}_{15}$ ceramics when $x \geq 0.3$.

5. CONCLUSIONS

The dielectric properties of investigated PMT-PT crystals are governed at lower temperatures (below 300 K) by polar nanoregions dynamics, while at higher temperatures (above 600 K) by electrical conductivity. The electrical conductivity occurs presumably due the hopping of oxygen vacancies and demonstrates the change in the activation energy close to 750 K temperature. The change in the activation energy can be explained by the increase of concentration of single ionized vacancies. The temperature dependence of the static dielectric permittivity was successfully described by the SBRF model with zero random fields and mean interaction energy 241 K. No anomaly in the temperature dependence of the static dielectric permittivity was observed in wide temperature range from 213 K to 950 K.

In samarium doped bismuth ferrite the ferroelectric phase transition temperature decreases with samarium concentration and finally no ferroelectric order is observed at $x = 0.2$. In contrast, the freezing temperature of relaxation processes at lower temperatures increases with samarium concentration. Finally, in ceramics with $x = 0.2$ the relaxor-like behaviour was observed. For middle concentration ($x = 0.15$) the antiferroelectric phase transition was observed. At higher temperatures (above 400 K) the dielectric properties of samarium bismuth ferrite ceramics are governed by Maxwell-Wagner relaxation and electrical conductivity. The DC conductivity increases and activation energy decreases with samarium concentration, especially at higher samarium concentrations.

$\text{Bi}_{1-x}\text{Dy}_x\text{FeO}_3$ ceramic is observed in two dielectric anomalies: the dielectric anomaly at low temperatures (below room temperature), which is caused by the dynamics of ferroelectric domains, while the dielectric anomaly at high temperatures (above 500 K) is caused by the electrical conductivity. $\text{Bi}_{1-x}\text{Dy}_x\text{FeO}_3$ ceramics electrical conductivity activation energy is characterized by electric transport of oxygen vacancies. With increasing concentrations of dysprosium decrease the DC conductivity and the conductivity activation energy increase.

Results of dielectric investigation of BIT and BGT revealed two different temperature regions of the dielectric dispersion. At higher temperatures (above 500 K) the dielectric spectra are dominated by electrical conductivity. It was proven that the compound demonstrated high ionic conductivity above T_0 and the electrical conductivity increased with increasing temperature. The activation energies are typical of the presumably oxygen vacancies migration-related conductivity. The results are of primary importance for understanding the peculiarities of conductivity behaviour in layered Aurivillius-type compounds. In the BGT, the behaviour at low temperatures is completely different – the dielectric anomaly, which could be associated with the domain like behaviour.

The broad dielectric anomaly in $\text{Ba}_2\text{NdFeNb}_4\text{O}_{15}$ is the sum of different relaxation processes. The dielectric spectra of $\text{Ba}_{6-2x}\text{Nd}_{2x}\text{Fe}_{1+x}\text{Nb}_{9-x}\text{O}_{30}$ ($x=0.6, 0.8, 1$) ceramics is typical of ferroelectric relaxors. In $\text{Ba}_2\text{NdFeNb}_4\text{O}_{15}$ ceramics the mean relaxation time of the low frequency process follows the Vogel-Fulcher law, while the mean time of high frequency process have anomalies close to the ferroelectric phase transition temperature. The activation energy increases with neodymium concentration.

$\text{Ba}_2\text{NdFeNb}_{3.7}\text{Ta}_{0.3}\text{O}_{15}$ solid solution exhibits dielectric anomalies typical of ferroelectrics and ferroelectric relaxors. Introduction of Ta^{5+} cations within the octahedral framework also causes the appearance of relaxor-like dielectric dispersion region in these TTBs and pushes ferroelectric phase transition to slightly lower temperatures. Despite these differences, cationic substitutions inside square channels and octahedral framework of these TTBs yield qualitatively to the same kind of dielectric behavior - ferroelectric to relaxor crossover. Since Ta^{5+} replaces ferroelectrically active Nb^{5+} cations and introduces additional disorder in these systems, it enables relaxor state expression in $\text{Ba}_2\text{NdFeNb}_{4-x}\text{Ta}_x\text{O}_{15}$ solid solutions by suppressing ferroelectric state. With increasing Ta^{5+} concentration the complete vanishing of ferroelectric state was observed together with considerable lowering of relaxor dispersion region temperatures.

REFERENCES

1. A. A. Bokov, Z. G. Ye, *Recent progress in relaxor ferroelectrics with perovskite structure*, Journal of Material Science **41**, 31-52 (2006).
2. M. A. Akbas, P. K. Davies, *Domain Growth in $Pb(Mg_{1/3}Ta_{2/3})O_3$ Perovskite Relaxor Ferroelectric Oxides*, J. Am. Ceram. Soc. **80**, 2933–36 (1997).
3. Z.G. Lu, C. Flicoteaux, G. Calvarin, *Dielectric and crystallographic study of the lead magnetantlate relaxor*, Materials Research Bulletin **31**, 445-452 (1996).
4. M. A. Akbas, P.K. Davies, *Processing and characterization of lead magnesium tantalate ceramics*, J. Mater. Res. **12**, 10 (1997).
5. A. Kania, *Flux growth of $Pb(Mg_{1/3}Ta_{2/3})O_3$ single crystals*, Journal of Crystal Growth **300**, 343 (2007).
6. A. Kania, *Flux Growth and Dielectric Studies of $(1-x) Pb(Mg_{1/3}Ta_{2/3})O_3 - xPbTiO_3$ Single Crystals*, Ferroelectrics **369**, 141-148 (2008).
7. A. Kania, A. Leonarska, Z. Ujma, *Growth and characterization of $(1-x) Pb(Mg_{1/3}Ta_{2/3})O_3 - xPbTiO_3$ single crystals*, Journal of Crystal Growth **310**, 594 (2008).
8. J. S. Kim, N. K. Kim, *Lead magnesium tantalate-lead titanate perovskite ceramic system: preparation and characterization*, Materials Research Bulletin **35**, 2479 (2000).
9. G. Catalan, J. F. Scott, *Physics and Applications of Bismuth Ferrite*, Adv. Mater. **21**, 2463 (2009).
10. S. Kamba, D. Nuzhnyy, M. Savinov, J. Sebek, J. Petzelt, J. Prokleska, R. Haumont, J. Kreisel, *Infrared and terahertz studies of polar phonons and magnetodielectric effect in multiferroic $BiFeO_3$ ceramics*, Phys. Rev. B **75**, 024403 (2007).
11. J.-C. Chen, J.-M. Wu, *Dielectric properties and ac conductivities of dense single-phased $BiFeO_3$ ceramics*, Appl. Phys. Lett. **91**, 182903 (2007).
12. A. K. Pradhan¹, Kai Zhang, D. Hunter, J. B. Dadson, G. B. Loitts, P. Bhattacharya, R. Katiyar, Jun Zhang, D. J. Sellmyer, U. N. Roy, Y. Cui, A. Burger, *Magnetic and electrical properties of single-phase multiferroic $BiFeO_3$* , JOURNAL OF APPLIED PHYSICS **97**, 093903 (2005).
13. S. Hunpratub, P. Thongbai, T. Yamwong, R.Yimnirun, S. Maensir, *Dielectric relaxations and dielectric response in multiferroic $BiFeO_3$ ceramics*, Appl. Phys. Lett. **94**, 062904 (2009).
14. K. S. Nalwa, A. Garg, *Phase evolution, magnetic and electrical properties in Sm-doped bismuth ferrite*, J. Appl. Phys. **103**, 044101 (2008).
15. S. Karimi, I. M. Reaney, Y. Han, J. Pokorny, I. Sterianou, *Crystal chemistry and domain structure of rare-earth doped $BiFeO_3$ ceramics*, J. Mater. Sci. **44**, 5102 (2009).
16. V. A. Khomchenko, J. A. Paixão, B. F. O. Costa, D. V. Karpinsky, A. L. Kholkin, I. O. Troyanchuk, V. V. Shvartsman, P. Borisov, W. Kleemann, *Structural, ferroelectric and magnetic properties of $Bi_{0.85}Sm_{0.15}FeO_3$ perovskite*, Cryst. Res. Technol. **46**, 238 – 242 (2011).
17. S. Pattanayak, R.N.P. Choudhary, P. R. Das, S.R. Shannigrahi, *Effect of Dy-substitution on structural, electrical and magnetic properties of multiferroic $BiFeO_3$ ceramic*, Ceramics International **40**, 7983–7991 (2014).

18. S.K. Barbar, S.Jangid, M.Roy, F.C.Chou, *Synthesis, structural and electrical properties of $Bi_{1-x}Dy_xFeO_3$ multiferroic ceramics*, *Ceramics International* **39**, 5359–5363 (2013).
19. Y. Li, J. Yu, J. Li, C. Zheng, Y. Wu, Y. Zhao, M. Wang, Y. Wang, *Influence of Dy-doping on ferroelectric and dielectric properties in $Bi_{1.052x}Dy_xFeO_3$ ceramics*, *J Mater Sci: Mater Electron* **22**, 323–327 (2011).
20. Y. Ding, J.S. Liu, H.X. Qin, J.S. Zhu, Y.N. Wang, *Why lanthanum-substituted bismuth titanate becomes fatigue free in a ferroelectric capacitor with platinum electrodes*, *Appl. Phys. Lett.* **78**, 4175 (2001).
21. L. Pintilie, M. Alexe, A.Pignolet, D. Hesse, *$Bi_4Ti_3O_{12}$ ferroelectric thin film ultraviolet detectors*, *Appl. Phys. Lett.* **73**, 342 (1998).
22. J. T. Dawley, R. Radspinner, R., B. J. J. Zelinski, D. R. Uhlmann, *Sol-Gel Derived Bismuth Titanate Thin Films with c-Axis Orientation*, *J. Sol-Gel Sci. Techn.* **20**, 85 (2001).
23. V.A. Khomchenko, G.N. Kakazei, Y.G. Pogorelov, J.P. Araujo, M.V. Bushinsky, D.A. Kiselev, A.L. Kholkin, J.A. Paixão, *Effect of Gd substitution on ferroelectric and magnetic properties of $Bi_4Ti_3O_{12}$* , *Mater. Lett.* **64**, 1066–1068 (2010).
24. J. L. Pineda-Flores, E. Chavira, J. Reyes-Gasga, A.M. Gonzalez, A. Huanosta-Tera, *Synthesis and dielectric characteristics of the layered structure $Bi_{4-x}RxTi_3O_{12}$ ($Rx=Pr, Nd, Gd, Dy$)*, *Journal of the European Ceramic Society* **23**, 839–850 (2003).
25. M. Josse, O. Bidault, F. Roulland, E. Castel, A. Simon, D. Michau, R. Von der Muhll, O. Nguyen, M. Maglione, *The $Ba_2LnFeNb_4O_{15}$ “Tetragonal Tungsten Bronze”: towards RT composite multiferroics*, *Solid State Sci.* **11**, 1118 (2009).
26. M. Kinka, M. Josse, E. Castel, S. Bagdzevicius, V. Samulionis, R. Grigalaitis, J. Banys, M. Maglione, *Ferroelectric and relaxor states in $Ba_2Pr_xNd_{1-x}FeNb_4O_{15}$ ceramics*, *IEEE Transactions on Ultrasonics, Ferroelectrics, and Frequency Control* **59**, 9 (2012).
27. F. Roulland, M. Josse, E. Castel, M. Maglione, *Influence of ceramic process and Eu content on the composite multiferroic properties of the $Ba_{6-2x}Ln_{2x}Fe_{1+x}Nb_{9-x}O_{30}$ TTB system*, *Solid State Sciences* **11**, 1709–1716, (2009).
28. M. Josse, P. Heijboer, M. Albino, F. Molinari, F. Porcher, R. Decourt, D. Michau, E. Lebraud, P. Veber, M. Velazquez, M. Maglione, *Original behaviours in $(Ba,Sr)_2Ln(Fe,Nb,Ta)_5O_{15}$ TTBs: anion-driven properties?*, *Cryst. Growth Des.* **14**, 5428–5435 (2014).
29. J. Grigas. *Microwave Dielectric Spectroscopy of Ferroelectrics and Related Materials*. Gordon and Breach publishers (1996).
30. J. Banys, S. Lapinskas, S. Rudys, S. Greicius, R. Grigalaitis, *High Frequency Measurements of Ferroelectrics and Related Materials in Coaxial Line*, *Ferroelectrics* **414**, 64-69 (2011).
31. D. Almond, G. K. Duncan, A. R. West, *The determination of hopping rates and carrier concentrations in ionic conductors by a new analysis of ac conductivity*, *Solid State Ionics* **8**, 159 (1983).
32. R. Pirc, R. Blinc, *Spherical random-bond–random-field model of relaxor ferroelectrics*, *Phys. Rev. B* **60**, 13470 (1999).

33. V. A. Khomchenko, J.A. Paixao, V.V. Shvartsman, P. Borisov, W. Kleemann, D.V. Karpinsky and A.L. Kholki, *Effect of Sm substitution on ferroelectric and magnetic properties of BiFeO₃*, Scripta Materialia **62**, 238–241 (2010).
34. Macutkevicius J, Banys J, Matulis A, *Nonlinear analysis: modeling and control* **9**, 75 (2004).
35. J. Macutkevicius, S. Kamba, J. Banys, A. Brilingas, A. Pashkin, J. Petzelt, K. Bormanis, A. Sternberg, *Infrared and broadband dielectric spectroscopy of PZN-PMN-PSN relaxor ferroelectrics: Origin of two-component relaxation*, Phys. Rev. B **74**, 104106 (2006).
36. R.H., Chen R.H., C.C. Yen, C.S. Shern, T. Fukami, *Impedance spectroscopy and dielectric analysis in KH₂PO₄ single crystal*, Solid State Ionics **17**, 2857 (2006).
37. A. Dziaugys, J. Banys, J. Macutkevicius, Yu. Vysochanskii, I. Pritz, M. Gurzan, *Phase transitions in CuBiP₂Se₆ crystals*, Phase Transitions **84**, 147 – 156 (2011).
38. U. T. Hochli, K. Knorr, A. Loidl, *Oriental glasses*, Advances in Physics **39**, 405 – 615 (1990).
39. M. Albino, P. Veber, S. Pechev, Ch. Labrugère, M. Velázquez, M. Maglione, M. Josse, *Growth and Characterization of Ba₂LnFeNb₄O₁₅ (Ln = Pr, Nd, Sm, Eu) Relaxor Single Crystals*, Cryst. Growth Des. **14**, 500–512 (2014).

AUTHOR'S PUBLICATION LIST

1. E. Masiukaitė, J. Banys, R. Sobiestianskas, T. Ramoska, V.A. Khomchenko, D.A. Kiselev, *Conductivity investigations of Aurivillius-type Bi_{2.5}Gd_{1.5}Ti₃O₁₂ ceramics*, Solid State Ionics **188**, 50 (2011).
2. E. Palaimiene, J. Banys, V.A. Khomchenko, K.Glemza, *Dielectric properties of Aurivillius-type Bi_{4-x}Gd_xTi₃O₁₂ ceramics*, Lithuanian Journal of Physics **53**, 210 (2013).
3. E. Palaimiene, J. Macutkevicius, J. Banys, A. Kania, *Dielectric properties of PMT-PT crystals*, Journal of Applied Physics **116**, 104103 (2014).
4. J.D. Bobić, M.M.Vijatović Petrović, N.I.Ilić, E.Palaimiene, R.Grigalaitis, C.O.Paiva- Santos, M.Cilence, B.D.Stojanović, *Lead-free BaBi₄Ti₄O₁₅ ceramics: Effect of synthesis methods on phase formation and electrical properties*, Ceramics International **41**, 309 (2015).
5. E. Palaimiene, J. Macutkevicius, D. V. Karpinsky, A. L. Kholkin, and J. Banys, *Dielectric investigations of polycrystalline samarium bismuth ferrite ceramic*, Applied Physics Letters **106**, 012906 (2015).
6. M. Kinka, D. Gabrielaitis, M. Albino, M. Josse, E. Palaimiene, R. Grigalaitis, M. Maglione, and J. Banys, *Investigation of Dielectric Relaxation Processes in Ba₂NdFeNb_{4-x}Ta_xO₁₅ Ceramics*, Ferroelectrics **486**, 1 (2015).

PARTICIPATION IN CONFERENCES

1. E. Masiukaitė, J. Banys, D. Kiselev, *Dielectric investigations of ferroelectric Bi_{2.5}Gd_{1.5}Ti₃O₁₂ ceramics*, 53rd Scientific Conference for Young Students of

- Physics and Natural Sciences, Open readings 2010, March 24 - 27, 2010, 61 - 62, Vilnius, Lithuania.
2. E. Masiukaitė, J. Banys, D. Kiselev, *Conductivity investigations of ferroelectric BGT ceramics*, 9th ISSFIT, June 1 - 5, 2010, 89, Riga, Latvia.
 3. **E. Masiukaitė**, J. Banys, V.A. Khomchenko, D.A. Kiselev, *Conductivity investigations of $Bi_{2.5}Gd_{1.5}Ti_3O_{12}$ ceramics*, Properties of ferroelectric and superionic systems: 3rd seminar, November 26 – 27, 2010, 19 - 20 Uzhgorod, Ukraine.
 4. E. Masiukaitė, J. Banys, V.A. Khomchenko, D.A. Kiselev, *Dielectric investigations of Aurivilius-type $Bi_{4-x}Gd_xTi_3O_{12}$ ceramics*, Conference of the COST MP0904 Action, EMF, June 26 - July 2, 2011, 166, Bordeaux, France.
 5. **E. Palaimienė**, J. Banys, V.A. Khomchenko, *Dielektriniai Aurivilijus struktūros BGT tyrimai*, 40-oji Lietuvos nacionalinė fizikos konferencija, June 10 - 12, 2013, Vilnius, Lithuania.
 6. R. Grigalaitis, P. Heijboer, Š. Svirskas, E. Palaimienė, J. Banys, M. Maglione, M. Josse, *Dielectric spectroscopy of TTB $Ba_{6-2x}Nd_{2x}Fe_{1+x}Nb_{9-x}O_{30}$ system*, COST SIMUFER Action MPO904 Workshop Advances in Ferroelectrics and Multiferroics, July 20 - 21, 2013, 37, Prague, Czech Republic.
 7. **E. Palaimienė**, J. Banys, V.A. Khomchenko, *Dielectric investigations of $Bi_3Gd_1Ti_3O_{12}$ ceramics*, dyProSo XXXIV 34th International Symposium on Dynamical Properties of Solids, September 15 - 19, 2013, 134, Vienna, Austria.
 8. **E. Palaimienė**, P. Heijboer, M. Maglione, M. Josse, R. Grigalaitis, J. Banys, *Dielectric properties of a new $Ba_{6-2x}Nd_{2x}Fe_{1+x}Nb_{9-x}O_{30}$ TTB system*, The Third Workshop for Early Stage Researchers of the COST MP0904 Action, November 6 - 9, 2013, 133, Novi Sad, Serbia.
 9. **E. Palaimienė**, P. Heijboer, M. Josse, M. Maglione, R. Grigalaitis, J. Banys, *Dielectric properties of $Ba_{6-2x}Nd_{2x}Fe_{1+x}Nb_{9-x}O_{30}$ ($x=0.6, 0.8$) tungsten bronze ceramics*, COST Action MP0904 - Closing Conference, January 30 – 31, 2014, Genoa, Italy.
 10. **E. Palaimiene**, R. Grigalaitis, D.V. Karpinsky, A.L. Kholkin, J. Banys, *Dielectric investigations of polycrystalline samarium bismuth ferrite ceramic*, Electroceramics XIV Conference, June 16 – 20, 2014, Bucharest, Romania.
 11. **E. Palaimiene**, J. Macutkevicius, A. Kania, J. Banys, *Dielectric properties of $0.9PbMg_{1/3}Ta_{2/3}O_3 - 0.1PbTiO_3$ single crystals*, European Conference on Applications of Polar Dielectrics (ECAPD-2014), July 7 - 11, 2014, Vilnius, Lithuania.
 12. **E. Palaimiene**, J. Macutkevicius, R. Grigalaitis, D.V. Karpinsky, A.L. Kholkin, J. Banys, *Conductivity investigations in multiferroic $Bi_{0.8}Sm_{0.2}FeO_3$ ceramics*, III Polish - Lithuanian – Ukrainian Meeting on Ferroelectrics Physics (PLU 2014), 31 August - 4 September, 2014, Wrocław - Pawłowice, Poland.

13. **E. Palaimiene**, J. Macutkevic, A. Kania, J. Banys, *Conductivity investigations of PMT-PT single crystals*, RCBJSF-2014-FMNT, September 29 – October 2, 2014, Riga, Latvia.
14. E. Palaimiene, J. Macutkevic, A. Kania, J. Banys, *Dielectric properties of PMT-PT crystals*, International Workshop on Relaxor Ferroelectrics (IWRF), October 12–16, 2014, 48, Stirin, Czech Republic.
15. E. Palaimiene, J. Macutkevic, D.V. Karpinsky, A.L. Kholkin, J. Banys, *Dielectric properties of samarium bismuth ferrite ceramic*, 2015 Joint IEEE International Symposium on Applications of Ferroelectric (ISAF), International Symposium on Integrated Functionalities (ISIF), and Piezoresponse Force Microscopy Workshop (PFM) (ISAF-ISIF-PFM 2015), May 24 - 27, 2015, Singapore.
16. A. Kirelis, E. Palaimiene, J. Macutkevic, J. Banys, D. Karpinsky, A. Kholkin, *Conductivity investigation in multiferroic $Bi_{1-x}Dy_xFeO_3$ ceramics*, 58th Scientific Conference for Students of Physics and Natural Sciences, Open Readings 2015, March 24 - 27, 2015, 208, Vilnius, Lithuania.
17. **E. Palaimiene**, J. Macutkevic, J. Banys, D.V. Karpinsky, A.L. Kholkin, *Conductivity investigations of multiferroic samarium bismuth ferrite ceramic*, 41-oji Lietuvos nacionalinė fizikos konferencija (LNFK-41), June 17 - 19, 2015, 308, Vilnius, Lithuania.
18. **E. Palaimiene**, J. Macutkevic, J. Banys, D.V. Karpinsky, A.L. Kholkin, *Dielectric investigations of polycrystalline dysprosium bismuth ferrite ceramic*, Functional Materials and Nanotechnologies (FM&NT-2015), October 5 – 8, 2015, Vilnius, Lithuania.
19. **E. Palaimiene**, J. Banys, A. Rotaru, F. D. Morrison, *Dielectric properties of $Ba_6MNb_9O_{30}$ ($M = Ga, Sc$) tungsten bronze ceramics*, IV Lithuanian-Ukrainian-Polish Meeting on Physics of Ferroelectrics (LUP IV), September 5-9, 2016, Palanga, Lithuania.

SANTRAUKA

Feroelektriniai relaksoriai – medžiagų grupė, dažniausiai turinti klasikinę perovskito struktūrą. Viena iš tokių medžiagų yra feroelektrinis relaksorius $0,94\text{PbMg}_{1/3}\text{Ta}_{2/3}\text{O}_3$ – $0,06\text{PbTiO}_3$ (PMT-PT) kristalas. Tiriant šį kristalą, buvo detaliau išnagrinėtos feroelektrinio relaksoriaus dielektrinės savybės. Ypač įdomus statinės dielektrinės skvarbos kitimas aukščiau kambario temperatūros, nes ši priklausomybė vis dar kelia mokslininkų diskusijų.

Medžiagų tyrėjai, ieškodami medžiagų, turinčių lengviau pritaikomų savybių, atkreipė dėmesį į bismuto feritą dėl jo feroelektrinių ir magnetinių savybių koegzistavimo. Tačiau bismuto ferito feromagnetinės savybės yra prastos ir nėra netinkamos taikyti, be to, jis pasižymi stipria nuotėkio srove. Norint pagerinti šios medžiagos savybes, dalis bismuto yra keičiama kitais retaisiais žemės elementais (pvz.: Nd, La, Sm, Dy). Samaris ir disprozis yra vienas iš variantų, keičiant koncentraciją $\text{Bi}_{1-x}\text{RE}_x\text{FeO}_3$ (RE = Sm, Dy) ar gaminimo metodu, yra ieškoma geriausių šių elementų elektrinių savybių. Tačiau įdedant priemaišų į feroelektriką, galimi įvairūs nepageidaujami scenarijai. Esant tam tikrai priemaišų koncentracijai, feroelektrinės savybės gali išnykti arba atsirasti nepageidaujama dipolinio stiklo arba relaksoriaus fazė. Plačiauostė dielektrinė spektroskopija yra nepakeičiama tiriant priemaišų įtaką feroelektrikų savybėms. Šiame darbe pirmą kartą parodyta, kad $\text{Bi}_{1-x}\text{Sm}_x\text{FeO}_3$ keramikose, kai $x = 0,2$, feroelektrinės savybės išnyksta ir atsiranda relaksoriaus fazė, o $\text{Bi}_{1-x}\text{Dy}_x\text{FeO}_3$ keramikose feroelektrinės savybės išlieka net kai $x \leq 0,2$, ir dielektriniai nuostoliai sumažėja.

Taip pat įdomios yra multiferoikų medžiagos, turinčios Aurivilijaus struktūrą, pavyzdžiui, sudarytos $\text{Bi}_4\text{Ti}_3\text{O}_{12}$ (BIT) pagrindu. Šios medžiagos yra aukšta Kiuri temperatūra (943 K), dėl kurios BIT yra plačiai taikomas elektriniuose elementuose, pavyzdžiui, energijos keitikliuose, pjezoelektriniuose atminties prietaisuose. Į BIT struktūrą buvo įterpta magnetinių savybių turinčio retųjų žemių metalo, pavyzdžiui, gadolinio (Gd). Šiame darbe pirmą kartą yra pateikiami medžiagų, t. y. $\text{Bi}_4\text{Ti}_3\text{O}_{12}$ ir $\text{Bi}_{4-x}\text{Gd}_x\text{Ti}_3\text{O}_{12}$ (BGT) ($x = 1$ ir $x = 1,5$), dielektriniai tyrimai. Parodyta, kad feroelektrinė tvarka neišnyksta BGT, kai $x = 1,5$, o dielektrinė dispersija yra nulemta feroelektrinių domenų dinamikos.

Ilgą laiką pagrindiniu tyrimų objektu buvo perovskito šeimai priklausančios keramikos. Dabar vis daugiau dėmesio sulaukia tetragoninės volframo bronzos, arba TTB medžiagų, kurių nėra labai daug, grupė. $\text{Ba}_2\text{REFeNb}_4\text{O}_{15}$ (RE = La, Pr, Nd, Sm, Eu, Gd) keramikos yra puikus įvairialypių TTB savybių pavyzdys. Junginiai su neodimiu, samariu ir europiu yra feroelektrikai, keramikos su praeodimiu ir gadoliniu pasižymi feroelektrinių relaksorių savybėmis, tačiau labai trūksta šių medžiagų dielektrinių tyrimų mikrobangų dažnių diapazone. Šiame darbe yra ištirtos medžiagų $\text{Ba}_2\text{NdFeNb}_4\text{O}_{15}$, $\text{Ba}_{6-2x}\text{Nd}_{2x}\text{Fe}_{1+x}\text{Nb}_{9-x}\text{O}_{30}$ ($x = 0,6$, $x = 0,8$), $\text{Ba}_2\text{NdFeNb}_{4-x}\text{Ta}_x\text{O}_{15}$ ($x = 0,3$, $x = 0,6$ ir $x = 2$) dielektrinės savybės ir fazinė diagrama.

Curriculum Vitae

Personal data

Name: Edita Palaimiene
Date of Birth: 1986 07 08
Place of Birth: Sirvintos, Lithuania
E-mail: edita.palaimiene@ff.vu.lt

Education

2005 – 2009 University first cycle (undergraduate, Bachelor) studies, Faculty of Physics (Modern Technologies Physics and Management), Vilnius University, Lithuanian.

2009 – 2011 University second cycle (graduate, Master's) studies, Faculty of Physics (Telecommunications Physics and Electronics), Vilnius University, Lithuanian.

2011 - 2016 PhD studies (Physical sciences, Physics), Vilnius University, Lithuanian.

Academic career

2010 – 2012 Engineer, Faculty of Physics, Vilnius University, Lithuanian.

2013 - up to now Lecturer and Junior scientific officer, Faculty of Physics, Laboratory of microwave spectroscopy, Vilnius University, Lithuanian.